ENCLOSURE 1

WESTINGHOUSE ADVANCED REACTORS DIVISION

CRBRP ENGINEERING STUDY REPORT

Number: ES-LRD-83-3029

Date: 2-10-83

Title: Sodium Slug Energy Absorption Capability of a Modified CRBRP Closure Head

Prepared by: W. E. Pennell — 2-10-83 (Date)

Approved by: W. W. Dewald — 2-10-83 (Date)

Distribution:
S. Additon (50)
W. W. Dewald
T. C. Varljen
C. G. Deese
P. W. Dickson
F. J. Baloh
J. E. Eck
P T. Falk
G. H. Nickodemus
J. W. Winters
L. E. Strawbridge

File No. 1-10-2-1

SUMMARY

SMBDB design requirements for the CRBRP closure head include a requirement for the head to accommodate the energy deposited by a 75MJ sodium slug. Tests on a 1/20 scale model of the closure head resulted in disengagement of the margin shear rings at pressures and deflections corresponding to a sodium slug energy of 40.8MJ. Investigation of the cause of the premature head failure revealed an unanticipated kinematic interaction between the deflected head plugs, which had the effect of disengaging the margin shear rings as head deflections increased.

Elimination of the kinematic failure mode can be accomplished by local machining of non-load bearing portions of head plugs and shield plates. In its modified configuration the head system has been shown to have the potential capacity to accommodate the energy from a 156MJ slug. The margin existing between the closure head predicted and required energy absorption capacities is considered more than sufficient to cover any uncertainties in the evaluation procedures. Confirmation of the energy absorption capability of the modified head will be obtained in additional hydrostatic and dynamic model tests.

TABLE OF CONTENTS

1. Introduction

Pressure loading produced by an HCDA event causes the sodium within the reactor vessel outlet plenum to be accelerated upward towards the closure head. The kinetic energy content of the slug at the instant of impact with the closure head is defined in Table 5-2 of Reference (1) at 75.1MJ. Static loading tests performed by SRI International on 1/20 scale models of the closure head (Reference (2)) indicate that the closure head would fail by plug disengagement pressure loading of 2010 psi. Integrating the area under the model closure head load deflection curve up to the collapse load limits defined by Table F-1322.2.1 of Reference (3) produced an allowable slug kinetic energy for the existing closure head design of 40.8MJ. Objectives for the design and analysis tasks summarized in this report were:

a. To determine the cause of the premature head failure,

b. Identify modifications which would increase the head failure load and associated energy absorption capability and,

c. Determine the slug energy absorption capability of the modified head.

2. Analysis of the SM-8 Model Closure Head Failure Mode

Deflection mode shapes for the SM-8 test are given in Figure 1. Model plug layouts were made corresponding to the deflection mode shapes. The layouts were made at 1/5 reactor scale (4 times model scale). The layout showed early closure of the gaps between the IRP and LRP on the lower surface of the head (see point 1 on Figure 2).

Premature closure of the gaps between plugs at the lower surface of the head introduced an unanticipated kinematic failure mode at the shear ring location. As the pressure increased beyond that associated with gap closure at point 1, further upward deflection of the plugs caused the IRP and LRP plugs to pivot about point 1. The pivoting action produces a lateral motion of the plugs at the elevation of the shear ring which ultimately leads to the shear ring becoming disengaged. Shear ring disengagement was the failure mode observed in the SM-8 tests.

Visual inspection of the component parts following the SM-8 test showed them to be in good condition with no evidence of structural failure. It follows, therefore, that the model had additional load carrying capability, were the premature kinematic disengagement of the shear ring to be eliminated. In this connection it is worth noting that the contacting surfaces at point 1 are in the non-load bearing portions of the head associated with the dip seal. It is possible, therefore, to eliminate the cause of the premature disengagement by locally machining the head to eliminate the interaction at point 1, without adversely impacting the structural strength of the individual plugs. This observation provides the basis for the closure head modifications evaluated in subsequent sections of this report.

It is important to note that the prying action associated with premature contact at point 1, results in an overall lateral motion of the entire IRP within the clearances provided in the LRP cavity. In the reactor closure head design this lateral motion would be resisted by 2 mechanisms. These are:

a. Shear stiffness of the riser assemblies which bridge the gaps between the rotating plugs and

b. Closure of the gaps between the margin shear ring keeper rings and the plugs once the plug lateral motion had exceeded the radial clearance at these locations. Neither the riser assemblies nor the margin shear ring keeper rings were represented in the SM-8 test. Failure in the SM-8 test would have been delayed to a higher pressure loading had these features been present. A preliminary evaluation of the effect of the missing features with the existing design, however, indicates that energy absorption capacity of the closure head would be less than the required 75MJ capacity.

It was concluded that modifications in the form of machining relief of the interferring portions of the closure head plugs and shield plates are therefore required. It is important however to recognize the effect of the risers and margin shear ring keeper rings in resisting lateral differential plug motions when assessing the effect of the proposed design modifications.

3. Modification Configuration Definition & Verification

The action plan used to:

a. Define configuration of the modified plugs and shield plates

b. Verify acceptable structural performance of the modified configuration and

c. Define the slug energy capability of the modified head design

is defined in Figure 3.

3.1 Configuration Definition

Extrapolation of the deflection mode shapes of Figure 1 to pressures beyond the 2010 failure pressure was done using individual node load deflection plots. Typical plots were shown in Figure 4. The plots can be divided into 3 sections. An initial section corresponds to largely elastic action of the plug assemblies. This section extends to ~1300 psi in Figure 4. Thereafter, the pressure deflection curve takes on a higher slope, indicating yielding of the plug material. The third section in which non-linear deflection of the plug is observed is associated with progressive disengagement of the margin shear rings. In the curves of Figure 4 this effect starts to become pronounced at pressures about 1800 psi and becomes dominant at 2010 psi.

The first two regimes in the curve can be related to bi-linear plug deformation. The plug strains at the instant of plug disengagement are still very much less than the limit of uniform elongation for the plug material. Plug deflection in the absence of premature disengagement can, therefore, be estimated by extrapolating the second portion of the load deflection curves. Samples of extrapolated curves are provided in Figure 5. A family of these extrapolated curves was used to define the deflected shape of the plugs at higher pressures.

The effect of disengagement at the shear ring connection is illustrated in Figure 6. At pressures in excess of 1600 psi, differential motion between the nodes on either side of the IRP-LRP gap becomes pronounced. The extrapolated curves did not include this element of plug deflection since the design modifications proposed delays plug disengagement such that it ceases to be a significant factor at loadings associated with the 75MJ slug. The non-linear disengagement effects were, however, considered in determining the ultimate energy absorption capability of the modified closure head.

Layouts of the closure head plugs were made at 1/5 scale for a range of pressure loadings. Layouts produced for 2700 psi and 3000 psi head loading are shown in Figures 7 and 8 respectively. The significance of these pressures is that 3000 psi conditions corresponds to the limiting shear strength of the LRP to reactor vessel joint, and the 2700 psi corresponds to the load which is permitted by the collapse load criteria of Reference (3).

Examination of Figures 7 and 8 shows interference between the IRP and LRP plugs and shield plates at the junction between nodes 9 and 10, interference between the IRP and SRP plugs and shield plates at the junction between nodes 5 and 6 and some interference between the LRP and the shear ring keeper ring at the junction between nodes 1 and 2. Machining modifications to the plugs and shield plates to eliminate the interference between the plugs and shield plates are shown in Figures 9 and 10. It is estimated from these figures that the machining modifications proposed do not influence the load carrying capability of the individual plug elements. The interference between the LRP plug and the existing shear ring keeper ring will inhibit rotation of the LRP ring and thereby increase engagement of the LRP-IRP shear rings. For this reason, the existing shear ring keeper rings will remain in their present configuration in the modified head. Head deflection profiles reflecting the effect of interaction between the LRP and the shear ring keeper ring are shown in Figures 11 and 12. The energy absorption capability of the head for these configurations is very slightly less than that associated with the configurations of Figures 7 and 8 due to a slight reduction in head deflection. ($\Delta E < 3\%$)

3.2 Limiting Shear Ring-Plug Geometry

Figure 2 shows the model plugs in the configuration corresponding to the failure pressure of 2010 psi. The IRP is shown at the extremes of lateral travel permitted by the inside diameter of the LRP. In one extreme of the travel the IRP ledge remains engaged with the margin shear ring, while at the other extreme no engagement remains. Visual examination of the model test pieces following the test show that they were not damaged in any significant way. This evidence suggests that the geometric condition existing in the model at the point of failure was that associated with lateral movement of the plugs such that complete disengagement had taken place. Based on this interpretation of the test data, geometric separation of the full scale plugs is considered acceptable provided that the remaining bearing and shear area is sufficient to carry the load of the plugs.

3.3 Limiting Pressure Retention Capability of the Modified Head

Analyses were performed to determine the limiting pressure retention capability of the closure head once modifications to eliminate the plug disengagement problem were in place. The shear joints between the plugs were identified as the limiting design features. Maximum shear loads occur in the LRP to reactor vessel shear joint. Limiting pressure retention capability of the closure head was therefore based on the shear strength of this joint.

The limiting shear strength of the LRP to reactor vessel joint was derived using the collapse load stress limits of Table F.1322.2-1 of Reference (3) coupled with materials dat taken from the individual component archive test results. A summary o the acceptance criteria and materials test data is provided in Figure 13.

The three potential shear planes in the LRP to reactor vessel shear joint are shown in Figure 14. The weakest of these shear planes is in the reactor vessel flange where flange shearout would limit the allowable pressure on the closure head to 2507 psi. This shear joint however is backed up by the outer riser bolted flange, which must also fail if the overall joint is to fail. The riser

flange strength is limited by the strength of its attachment studs. Analysis summarized in Figure 15 shows that an additional 248 psi would be required to fail the flange studs. The allowable load on the LRP to reactor vessel joint therefore is obtained as 2507 + 248 = 2755 psi.

The acceptance criteria adopted in the analysis of the shear joint strength limit the allowable load to 90% of that which would cause failure. The predicted failure load would therefore be 2755/0.9 = 3060 psi. Layouts of the head deformed configuration were therefore made for pressures of 2700 and 3000 psi.

3.4 Limiting Plug Gap Reductions

One of the parameters considered for modification was the radial gap between the plug and the margin ring key ring. Closing this gap would limit the ability of the IRP to move laterally within the LRP, and thereby contribute to the delay of shear joint disengagement. The present definition of the design modifications does not include the reduction in this gap. The summary of the evaluations performed to determine the miniminum acceptable gap however is provided in Figures 16-19. The evaluations showed that a minimum gap of 1/8 of an inch would permit free running of the plugs during normal operation and would have no impact on the seismic response of the closure head.

3.5 Plug Strains

An evaluation of the plug strains is important to

a. Verify that the plug is operating in the stable region of the post yield stress-strain curve and,

b. Verify that the plug strains are not approaching a level at which failure due to strain exhaustion is possible.

An evaluation of the plug strains is provided in Figure 20. Geometric data required to determine the strain levels in the main body of the plugs were obtained from the head deformed layout drawings. Maximum

strains occur at the free edges of the plugs and are therefore uniaxial in nature. The maximum strain was found to be 1.2%. The uniaxial elongation for the head structural material at the operating temperature of 400°F is 7%. This strain level is equated to the plastic instability strain of Reference (3). The allowable strain is limited to 0.7 of the plastic instability strain. The allowable strain is therefore .7 X 7.0 = 4.9%. The maximum strain in the body of the plug is therefore seen to be approximately 25% of the allowable strain. The load deflection characteristics of the plugs at this relatively low post yield strain level will be stable.

It is to be expected that some of the highest strains in the head system will be found in the shear joints where the loads are concentrated. The LRP to reactor vessel shear joint was subject to a shear load corresponding to a 2587 psi pressure load on the head during the SM-7 tests. While the stiffness of the plugs in the SM-7 test was not prototypic, representation of the shear joints was prototypic. The SM-7 tests therefore provided a valid proof test on the LRP to reactor vessel shear joint. The joint did not fail during the test. While the test verification pressure of 2587 psi is lower than the predicted limit pressure strength of the head, it is higher than the pressure strength required to demonstrate the capability to absorb the kenetic energy from a 75.1MJ slug. (The required pressure retention capability for a 75.1MJ slug is derived in Section 4 as 2180/0.9 = 2420 psi).

4. Energy Absorption Performance of the Modified Head

In order to define the slug energy absorption capability of the modified head it is first necessary to define the percentage of the slug energy expended in performing work on the closure head. The kinetic energy in the combined slug-head mass immediately following the impact is related to the slug kinetic energy immediately prior to impact by the law of conservation of momentum. Given a slug mass of 0.368×10^6 lb and a head mass of 1.046×10^6 lb, the energy imparted to the head is approximately 19.5MJ. A summary of the derivation of this value is provided in Figure 21.

In order to have confidence that the estimated energy imparted to the head is a reasonable value the energy converted from kinetic energy to potential energy within the sodium slug is investigated as an example of the post impact energy location.

Pressure and flow conditions within the slug in the period immediately following the slug impact can be estimated using conventional waterhammer analysis for flow in pipes with an instantaneous gate closure. The sequence of events in the fluid immediately following gate closure (slug impact) is illustrated in Figure 22, extracted from Reference (4). A pressure wave is seen to travel down the length of the fluid slug, leaving the entire slug pressurized at the peak impact pressure at time $t = 1/a$ seconds. The impact pressure associated with 75MJ slug in a vessel with no UIS present is obtained from the SM-2 dynamic model test as 5300 psi (Reference (5)). The bulk modulus required to calculate the volumetric contraction of the slug, and the potential energy stored in the compressed slug was obtained from Reference (6). The calculation of the potential energy stored in the compressed slug is provided in Figure 23. The stored energy is obtained as 39.6MJ or 53% of the original slug kinetic energy content.

The closure head and slug between them thus account for approximately 79% of the slug energy in the period immediately following impact. Energy storage mechanisms such as vessel wall straining, re-directed slug flow and slug turbulence account for the balance of the slug energy. Table 5-2 of Reference 1 shows that much of the slug energy is ultimately deposited in the reactor vessel wall.

Work performed in deflecting the SM-8 test head up to the configuration corresponding to its 2010 psi failure pressure can be obtained by integrating the area under the pressure-volume change curve given in Reference (2). The curve from Reference (2) is reproduced in Figure 24 of this report. The integral under the SM-8 curve up to the point of failure gives an energy absorption capability of 200×10^6 in lb. The acceptance criteria of Reference (3) however limit the maximum permissible loads to 90% of the failure loads. The indicated maximum usable energy absorption capability of the existing head is therefore limited to that associated with a head pressure of $0.9 \times 2010 \cong 1800$ psi. Integration of the test pressure-volume change curve over the pressure range zero to 1800 psi yields a usable head work value of 94×10^6 lb in. Using the value derived in Figure 21 for the energy deposited in the head by a 75MJ slug (173×10^6 lb in), the predicted slug energy capability of the existing closure head design is obtained as 40.8MJ.

It was shown in Section 3 of this report that the failure pressure for the modified closure head is approximately 3000 psi. With this failure pressure, the allowable maximum pressure on the closure head is $0.9 \times 3000 = 2700$ psi. The pressure-volume curve from the SM-8 test can be extrapolated to the higher failure pressure provided the mode of plug motion in the disengagement phase of the head loading is known. If the plugs start to disengage, the pressure-volume change curve flattens as failure is approached, giving an increase in the total energy absorbed for a given maximum pressure load on the head. With no plug disengagement, a straight line extrapolation of the pressure-volume change curve is obtained. This mode of extrapolation results in a lower bound estimate of the energy absorption capability of the closure head for a given maximum pressure loading. A comparison of

the model plug shear ring configuration at failure (Figure 2), with the shear ring configuration at 3000 psi loading in Figures 8 and 12 indicates that there should be little non-linear plug disengagement motion at 3000 psi loading. Information on the energy absorption capacity at failure with non-linear plug disengagement is useful however in that it indicates the energy abosorption margin available should unanticipated non-linear plug disengagement effects be encountered. Both linear and non-linear extrapolation curves are provided in Figure 24. Note that while the volume change at failure for these curves differ significantly (points 1 and 2), the curves yield similar results at the maximum pressure permitted by the acceptance criteria (points 3 and 4).

Integrating the area under the pressure-volume change curve to points 1 and 2 gives estimates of the energy absorbed at failure of 464 X 10^6 lb in (201MJ) for the case of non linear disengagement (NLD) and 394 X 10^6 lb in (171MJ) for the case of no non-linear disengagement. Comparing these results with the test result for the original head configuration the energy absorbed at failure is seen to have been increased by 132% for the NLD mode and 97% for the no NLD mode.

At the limiting collapse load pressure (0.9 X failure pressure) the energy absorbed by the modified head in the NLD mode is 314 X 10^6 lb in (136MJ) (point 3) and 308 X 10^6 lb in (134MJ) point 4) in the no NLD mode. This compares with a predicted energy absorption of 94 X 10^6 lb in (40.8MJ) for the existing head design at the limiting collapse load pressure of 1800 psi (point 6). The head modifications have therefore increased the head energy absorption capacity at the limiting collapse load pressure by 234% and 227% for the NLD mode and no NLD modes respectively.

Work absorbed by the closure head as derived from an extrapolation of the SM-8 model test curves is summarized in Figure 25.

A number of small additional sources of slug energy absorption exist in the reactor head and support system. Lifting the mass of the head as the head deforms upwards contributes 5 X 10^6 lb in of potential energy. Dynamic response of vessel support system (vessel flange, attachment bolts and the steel ledge) due to out of balance SMBDB inertia loads produces a 0.43 inch upward motion of the head support. This motion consumes 11 X 10^6 in lb of strain energy. The analytical model, loads, and vessel flange response used to derive support system energy absorption are shown in Figures 26 through 29.

A final correction is required to account for differences between the pressure area used in the SM-8 model and that existing in the actual closure head under SMBDB pressure loading. The pressure seal bladder is shown in Figure 1 to extend to a model radius of the vessel I.D. In the closure head however the SMBDB pressures would extend outwards to the LRP margin shear ring. Extending the pressure out to the radius and multiplying the resulting load by the small deflection of this area under 2700 psi loading results in an addition of 38 X 10^6 lb in to the head work integral.

A summary of the head system energy absorption capability is provided in Figure 30.

5. Evaluation

Entering the head energy absorption curve of Figure 25 with the energy deposited in the head by a 75MJ slug, the required pressure load capacity of the head is estimated as 2180 psi. The allowable pressure load on the modified head has been calculated to be 2700 psi. The reserve factor on head strength (RF) is therefore obtained as follows.

$$RF_s = \frac{2700}{2180} = 1.24$$

The lower bound energy absorption capacity of the modified head system is obtained from Figure 30 as 360×10^6 lb in. The energy deposited in the head system by a 75MJ slug is estimated in Figure 21 as 173×10^6 lb in. The reserve factor on energy (RF_E) absorption at the maximum allowable pressure for the modified head is therefore:

$$RF_E = \frac{360 \times 10^6}{173 \times 10^6} = 2.08$$

The controlled parameter is the energy content in the slug at the instant of contact with the head (75MJ). The reserve factor of 2.08 obtained for the energy absorption capacity of the modified head is considered more than adequate to cover any uncertainties in the evaluation procedure.

The reserve factor on head strength is considered adequate at 1.24. An important consideration in arriving at this conclusion is the demonstration in SM-7 test of a shear strength capability well in excess of that required for the absorption of a 75MJ slug (2580 psi in the test vs a required pressure of 2180 psi).

Experience has shown that the most satisfactory means of assessing the SMBDB energy absorption capacity of the closure head is by test. A hydrostatic test of the modified head geometry is planned to confirm that all interferences which contributed to the kinematic failure mode have been satisfactorily eliminated. This will be followed by a confirmatory dynamic test using the scale equivalent of a 75MJ slug.

6. Conclusion

Kinematic interaction between the head plugs has been identified as the cause of premature disengagement of the plugs during the SM-8 test. Local machining of the non-load bearing portions of the head plugs and shield plugs has been shown to eliminate the interferences which caused kinematic disengagement of the margin shear rings. With the

elimination of the kinematic failure mode, the modified head has a potential capacity to accommodate the energy from an approximately 150MJ slug. The SMBDB design requirement for the closure is that it accommodate the energy from a 75MJ slug. The margin existing between the potential energy absorption capacity of the modified head and the required energy absorption capacity is more than sufficient to accommodate the uncertainties in the evaluation.

Finalization of the head machining modifications and confirmation of the head energy absorption capability will be obtained in additional hydrostatic and dynamic model tests.

7. References

1. Hypothetical Core Disruptive Accident Considerations in CRBRP, Volume 1: Energetics and Structural Margin Beyond the Design Base.

2. Static Tests of 1/20-Scale Models of the Clinch River Breeder Reactor Head in Support of the LMFBR Safety Program, C. M. Romander and Y.D. Murray; A. L. Florence, Project Supervisor, December 1982.

3. Section III, Division 1, Appendix F of the ASME Boiler and Pressure Vessel Code.

4. Watterhammer Aanlysis, John Parmakian, 1963.

5. Structural Response of 1/20-Scale Models of the Clinch River Breeder Reactor to a Simulated Hypothetical Core Disruptive Accident (SRI International), C. M. Romander and D. J. Cagliostro; A. L. Florence, Project Supervisor, October 1978.

6. Nuclear Systems Materials Handbook, Volume 1, Design Data, Property Code 3307.

7. Evaluation of Coolant Impact Effects on the Reactor Cover, A. H. Marchertas, Y. W. Chang, and S. H. Fistedis, ANL 7987, November 1972.

8. Dynamic Structural Response of LMFBR Head Closures to Hypothetical Core Disruptive Accidents, Nuclear Engineering and Design, 49 (1978) 119-12, R. F. Kulak, Argonne National Laboratory.

APPENDIX A

A review of additional information was performed to determine the appropriateness of characterizing the energy imparted to the head assuming purely inelastic slug behavior. The results of the review are summarized below.

I. Parametric Calculations Using REXCO

Argonne National Laboratory (ANL) performed a sensitivity study in 1972 to determine energy delivered to the head as a function of reactor vessel wall thickness (Reference 7). The FFTF configuration, which is similar to CRBRP, was used as the basis for the study. Although ANL showed that the energy delivered might be in the range of 25 percent greater than that from a purely inelastic collision, their conclusion was:

"The approximation of inelastic collision in deriving the energy [delivered to the head] is quite good for relatively thin vessels."

II. Evaluation of SRI Test Data

There is a question regarding the validity of slug velocities measured in the SM-2 and SM-5 tests. Nevertheless, the reported velocities were evaluated to determine the degree to which the slug impact was elastic. Any relative head/slug motion immediately after impact would suggest that there was energy delivered to the head in excess of that calculated assuming an inelastic collision. The evaluation indicated that the elastic component in the collision was small; the indicated head energy would be less than 10 percent greater than the inelastic energy.

III. Detailed Head Response Evaluation

Argonne National Laboratory (ANL) performed a detailed evaluation of the CRBRP head response to SMBDB loadings in 1978 (Reference 8). The under-head loadings predicted by REXCO were used as input to the evaluation. (No consideration was given to the potential disengagement failure mode.) Extrapolation of the ANL results considering any one of 3 different methods [1) predicted displacement vis-a-vis head stress-strain characteristics, 2) the integral of pressure over distance due to head motion, and 3) predicted displacement vis-a-vis displacement-static pressure characteristics determined from test SM-8) suggests that substantially less than 20 MJ would be imparted to the head.

Conclusion

Although there is some uncertainty regarding the amount of energy that will be imparted to the head, the energy estimated using the inelastic collision model is a reasonable estimate. The residual uncertainty is readily accommodated by the large margins in predicted head structural capability identified in Section 6.

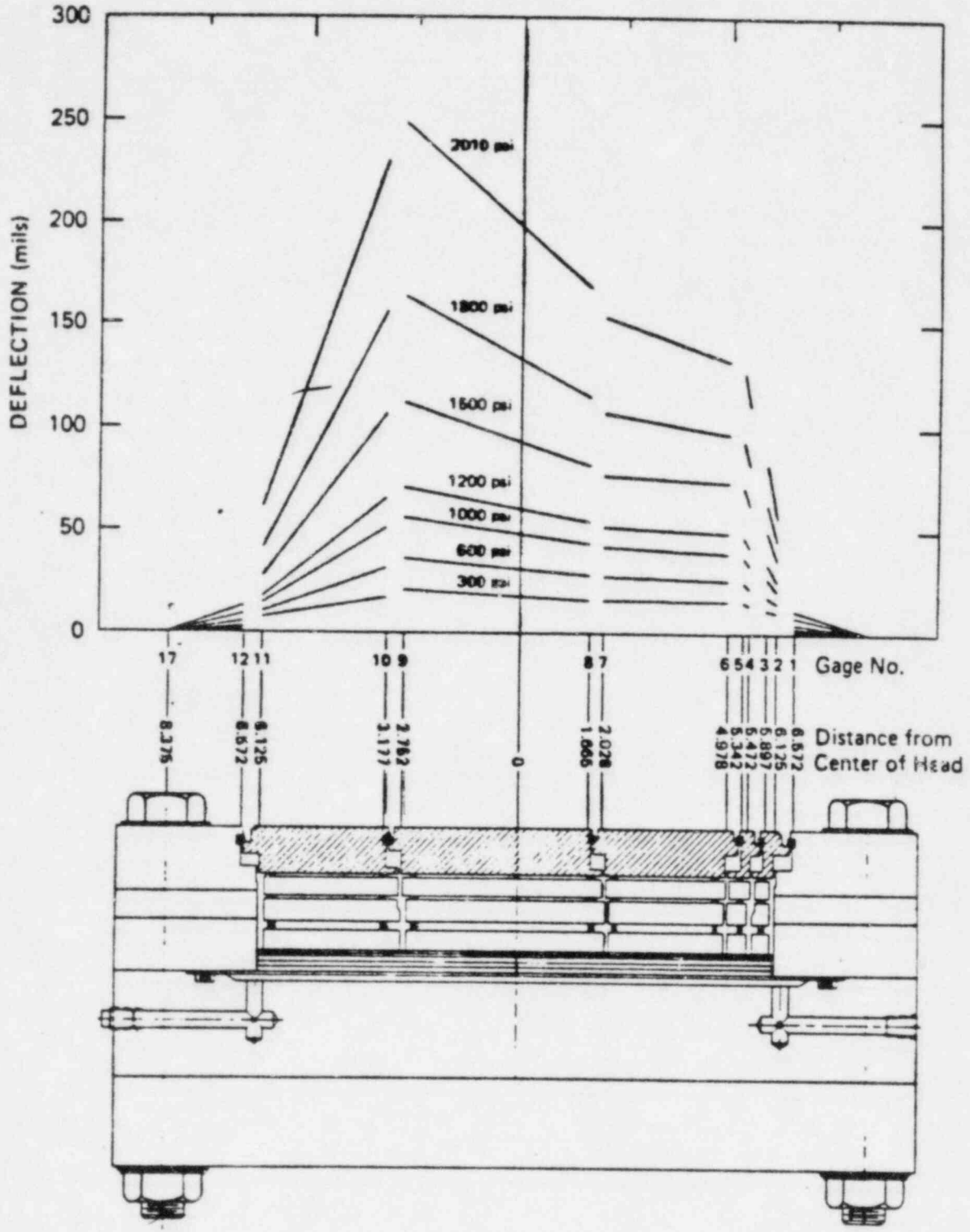

Figure 1
Profiles of Head at Seven Pressures on SM 8

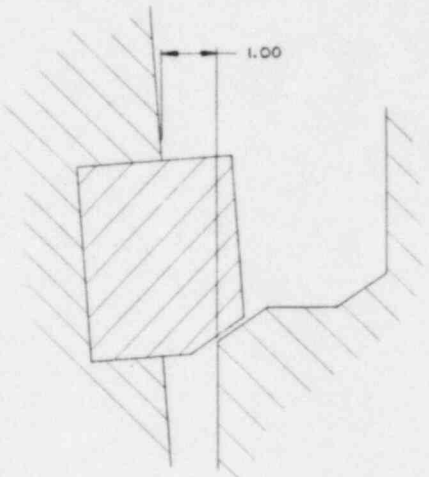
1.00

DETAIL A

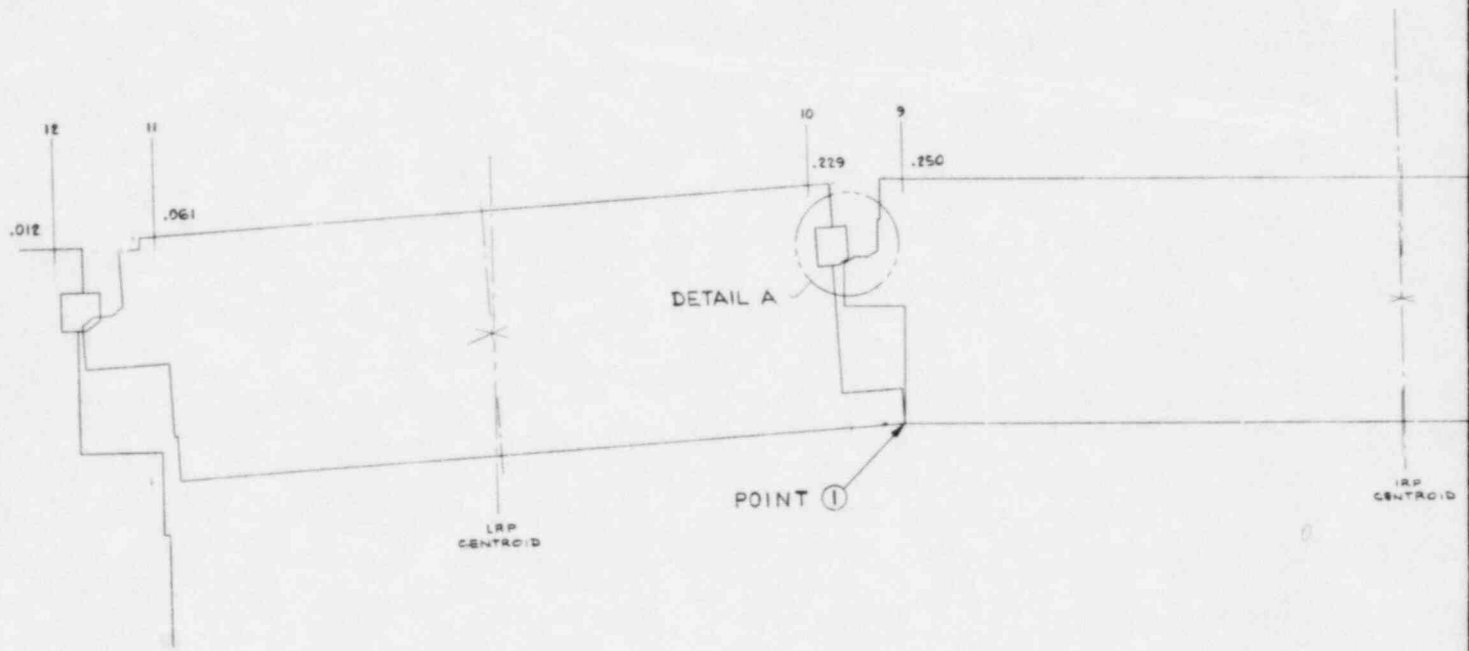
12
11
10
9
.012
.061
.229
.250
DETAIL A
POINT (1)
LRP CENTROID
LRP CENTROID

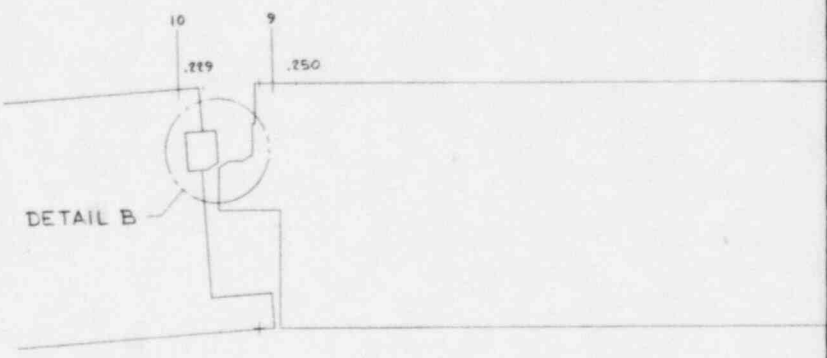
10
9
.229
.250
DETAIL B

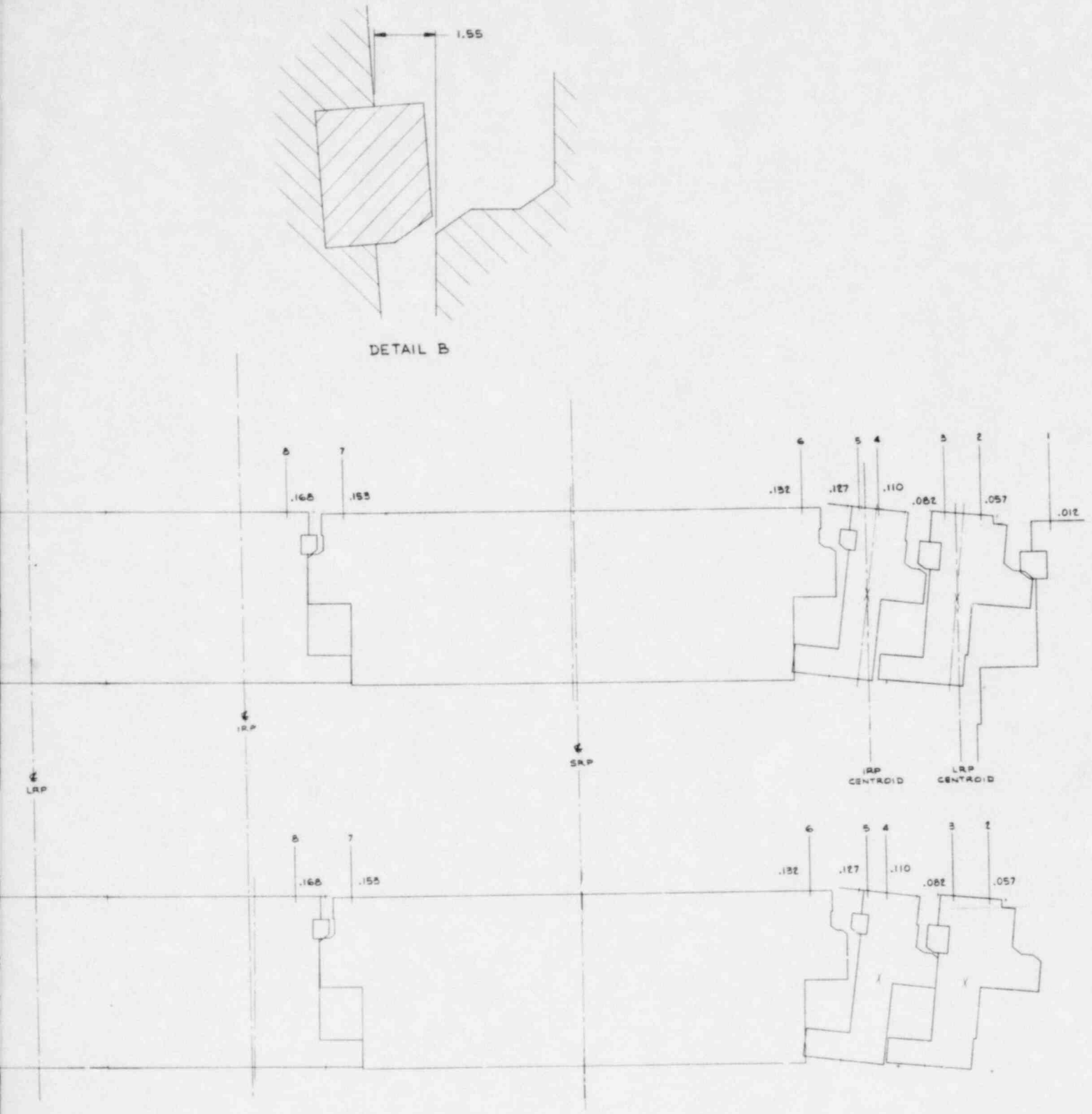

SM-8 MODEL
PLUG CONFIGURATION
AT FAILURE (2010 PSI)

FIGURE 2

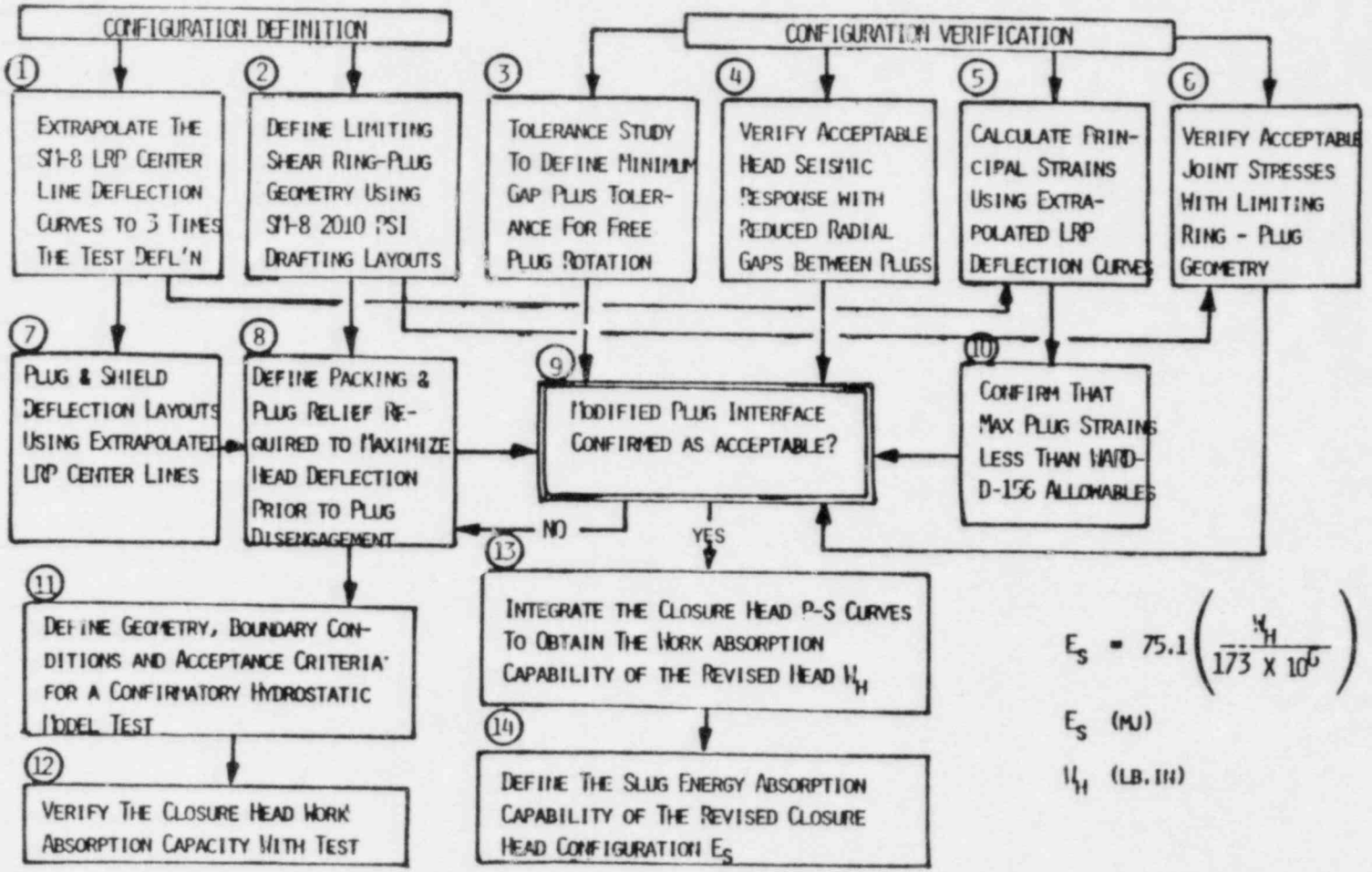

Figure 3
Design Modification Logic CRBRP Closure Head SMBDB Capacity Enhancement

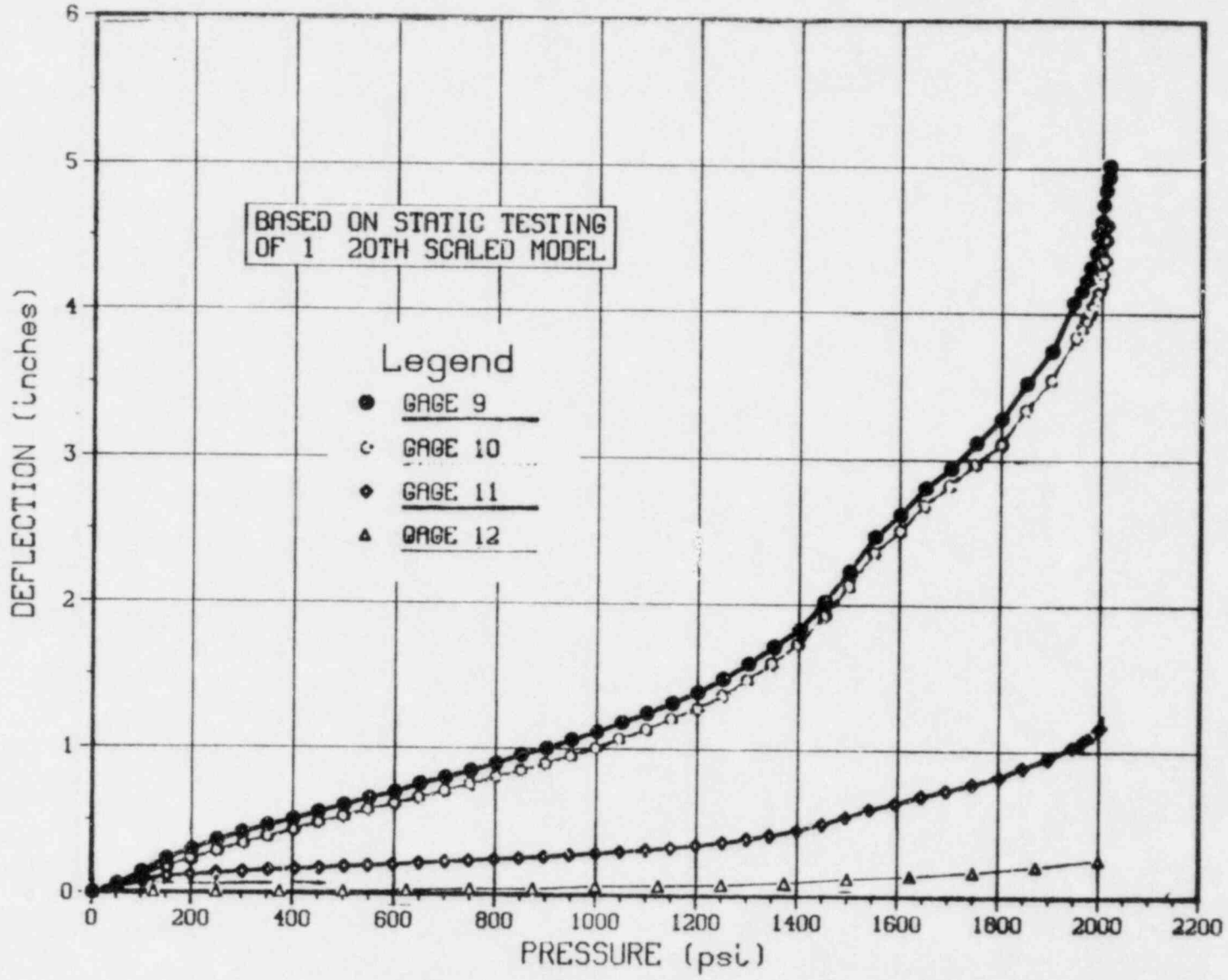

Figure 4
CRBR RV and Rotating Plugs Absolute Displacements Due to HCDA

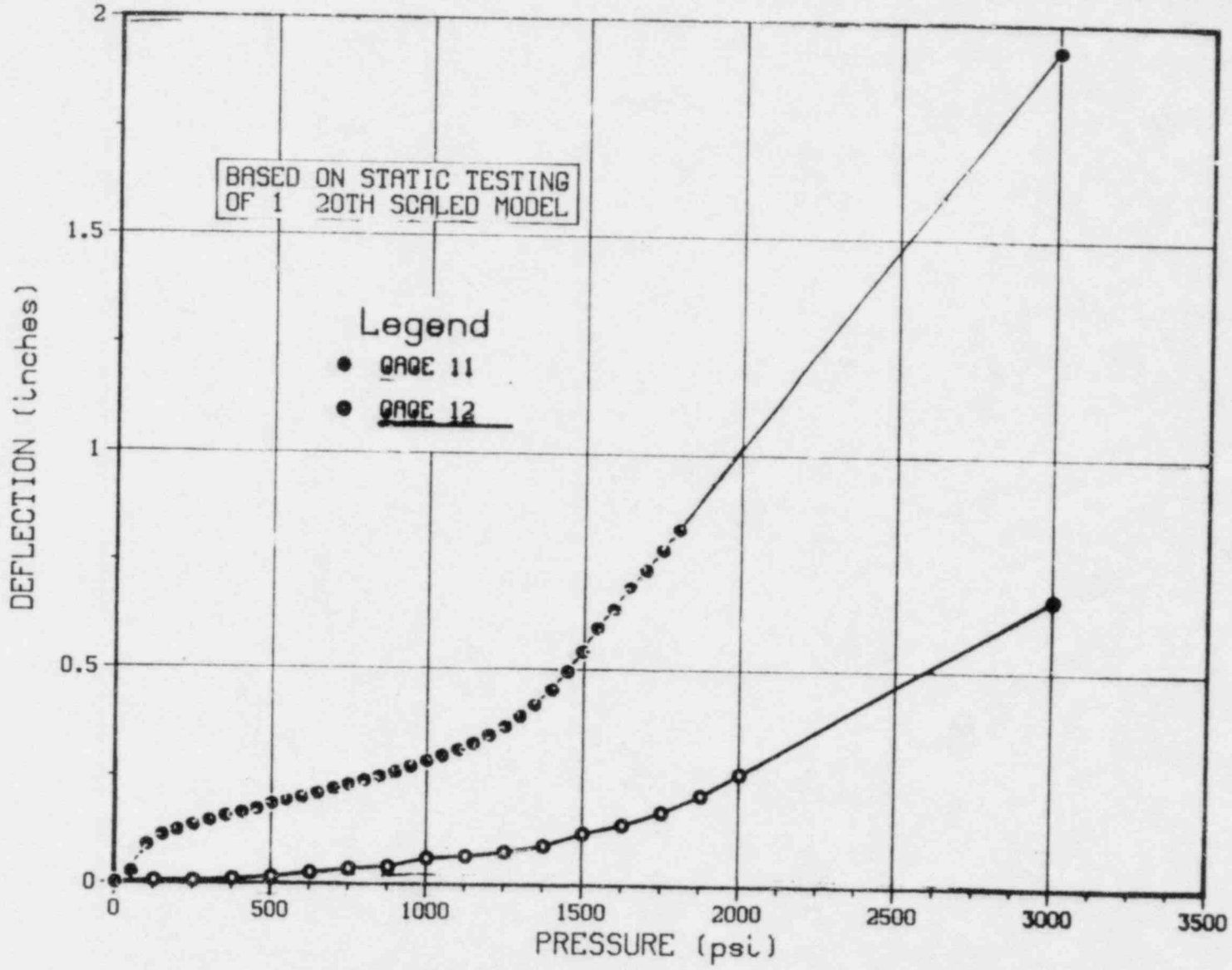

Figure 5
CRBR RV and Rotating Plugs Absolute Displacements Due to HCDA

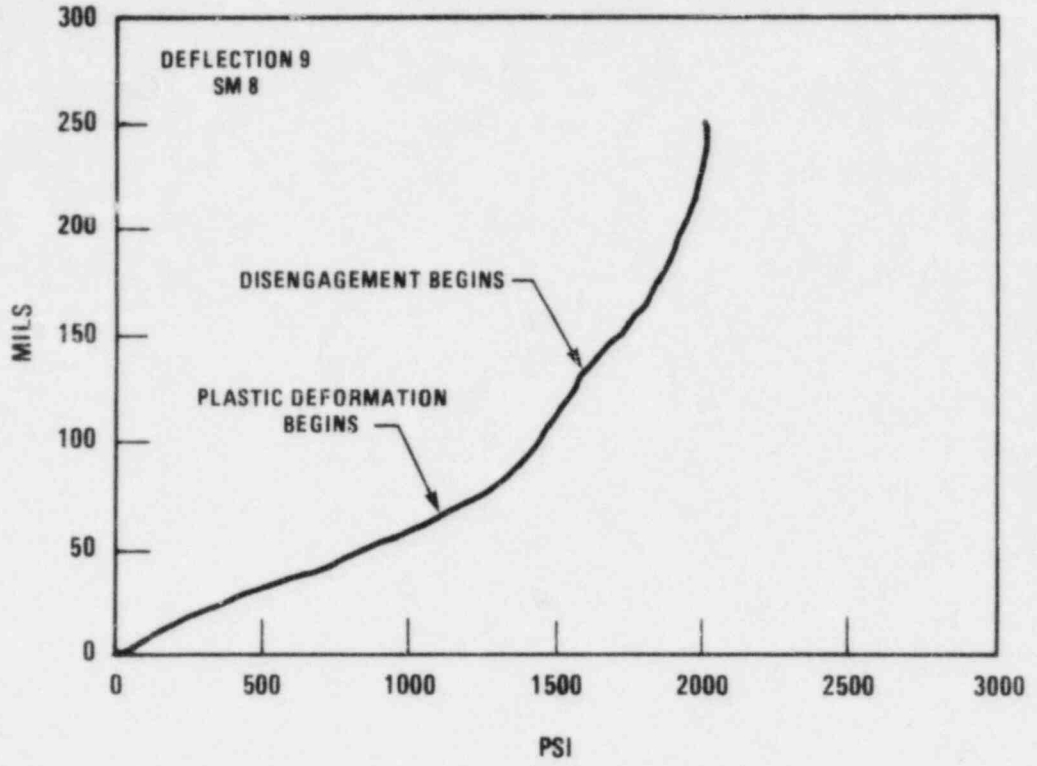

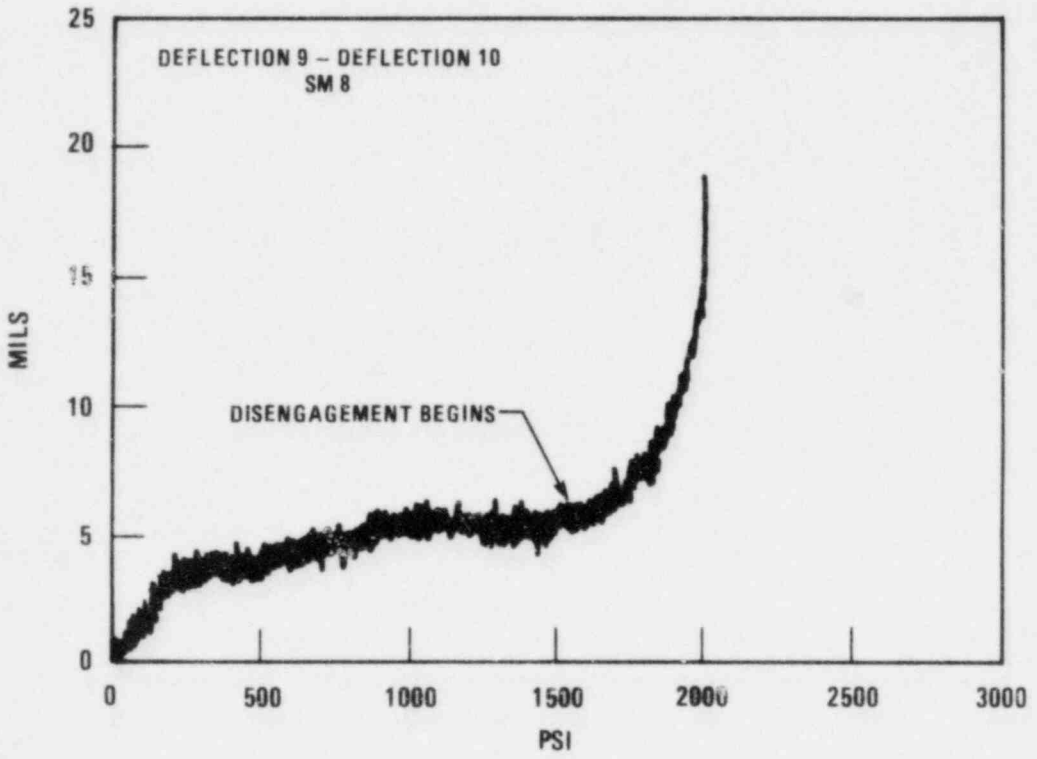

Figure 6
Relative Displacements Across Point of Disengagement for Tests SM 7 and SM 8

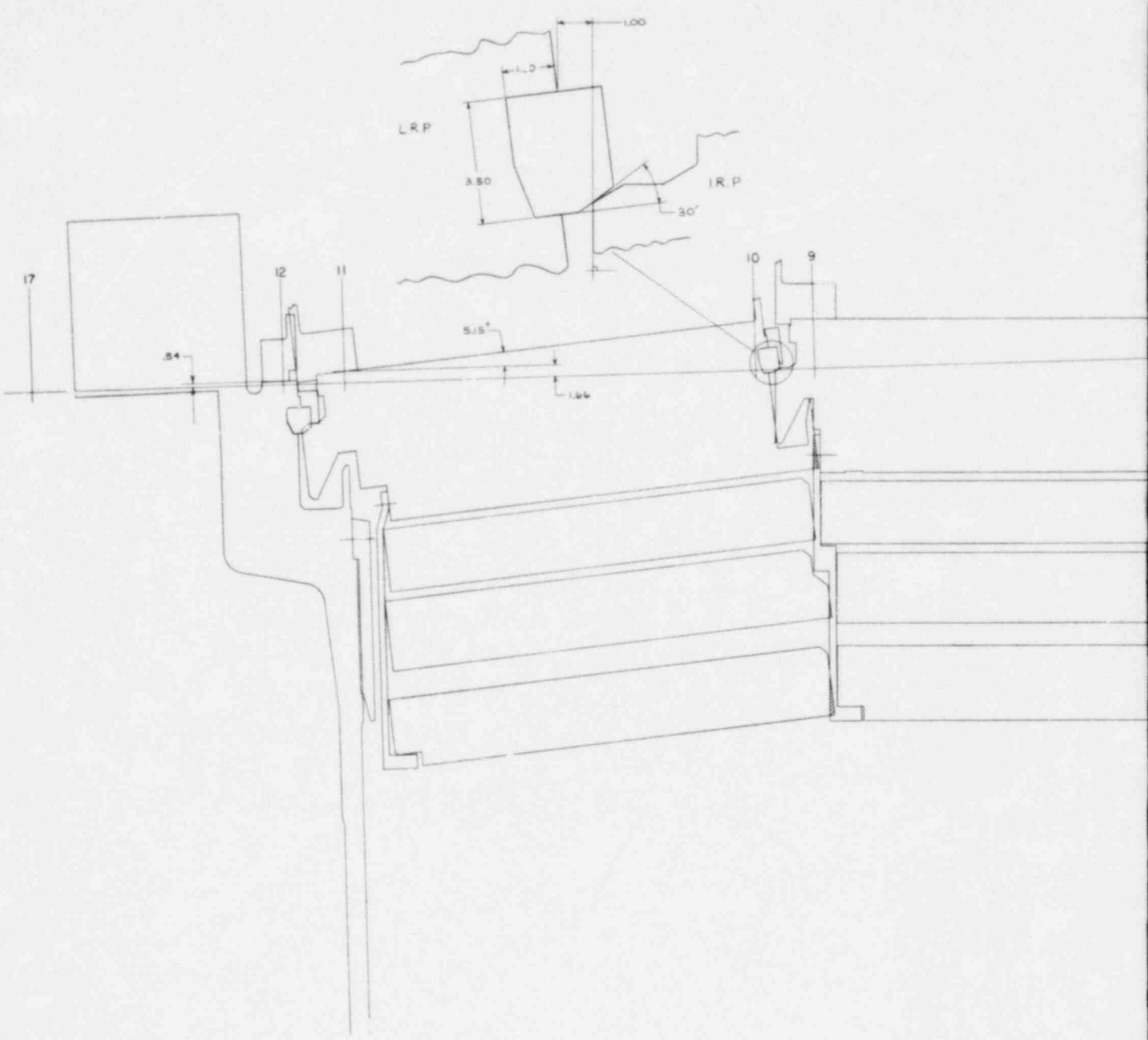
1.00
1.0
L.R.P
3.50
I.R.P
30°
17
12
11
10
9
.84
5.15°
1.66

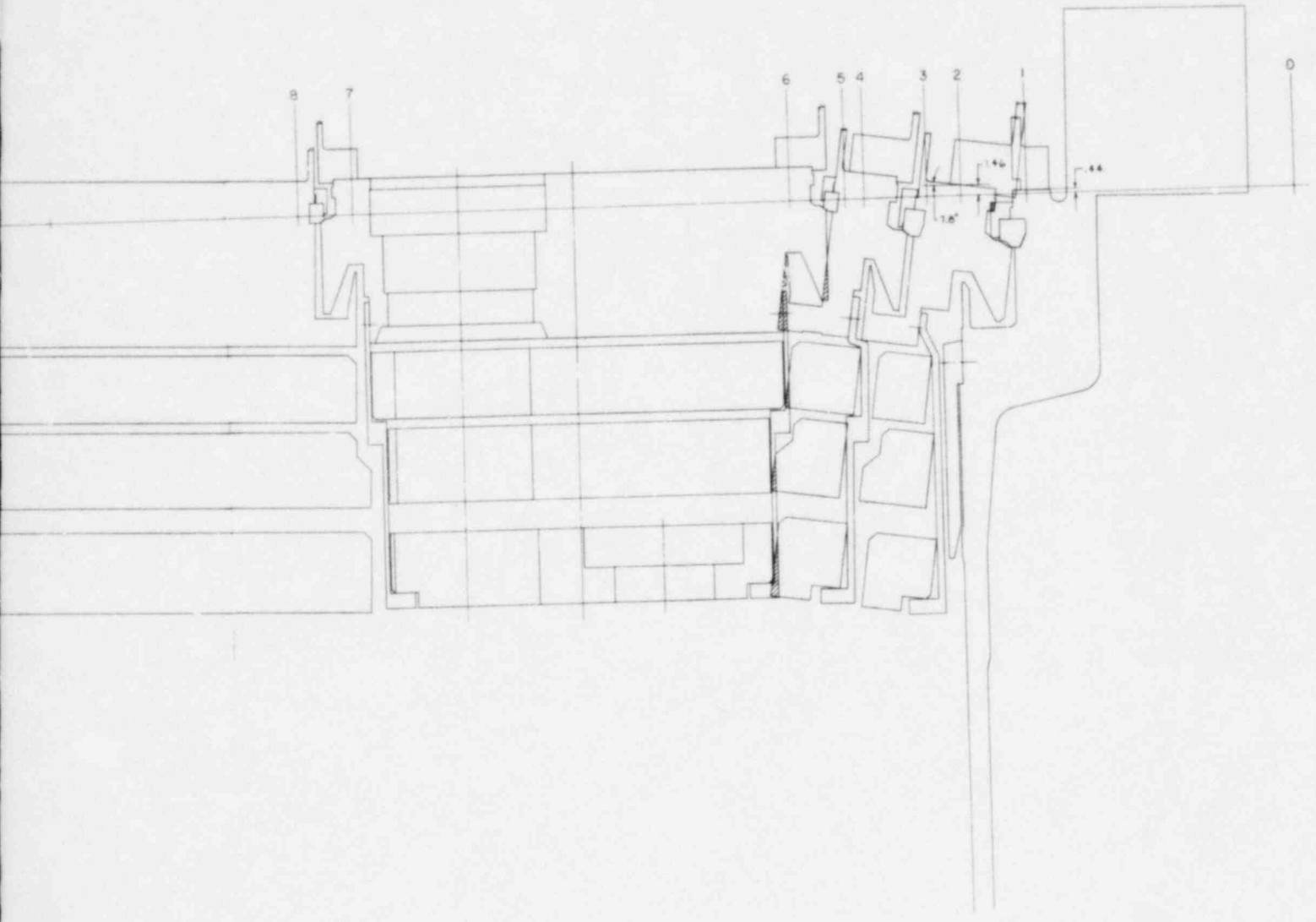

PROJECTED CLOSURE HEAD
DEFLECTIONS AND INTERFERENCES
AT 2700 PSI

FIGURE 7

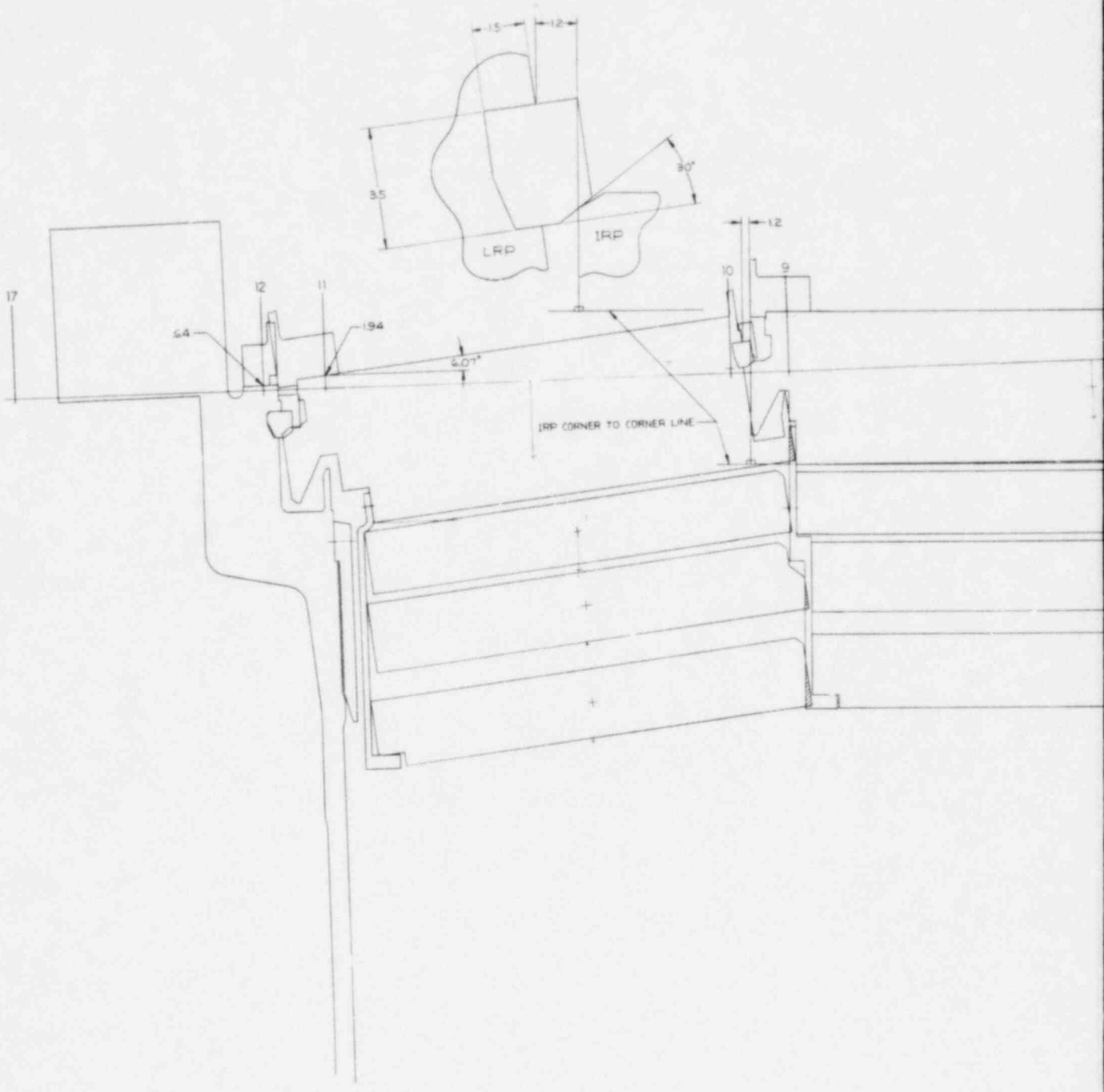
.15
.12
3.5
30°
LRP
IRP
.12
10
9
17
12
11
.64
.194
4.07°
IRP CORNER TO CORNER LINE

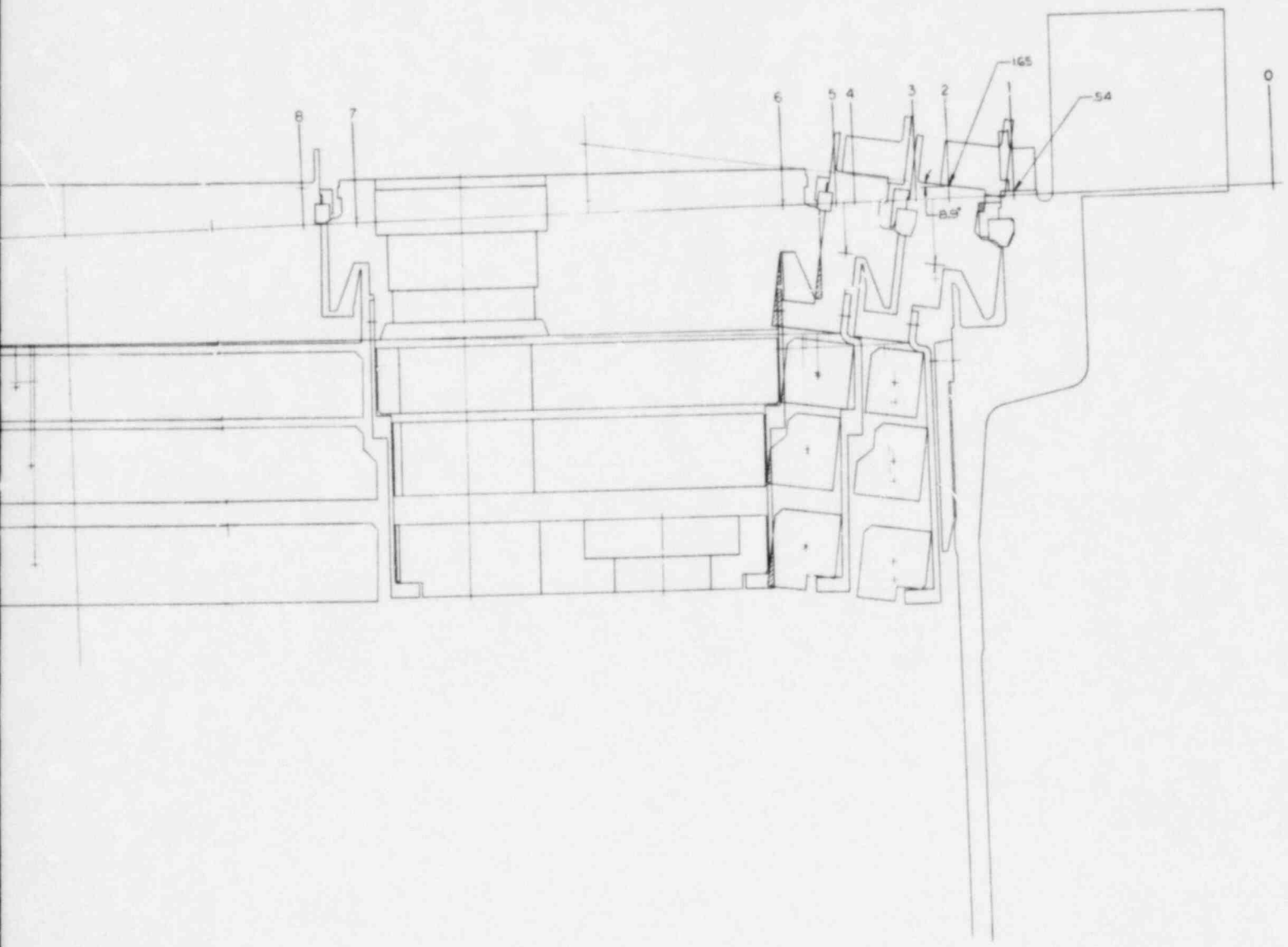

PROJECTED CLOSURE HEAD
DEFLECTIONS AND INTERFERENCES
AT 3000 PSI

FIGURE 8

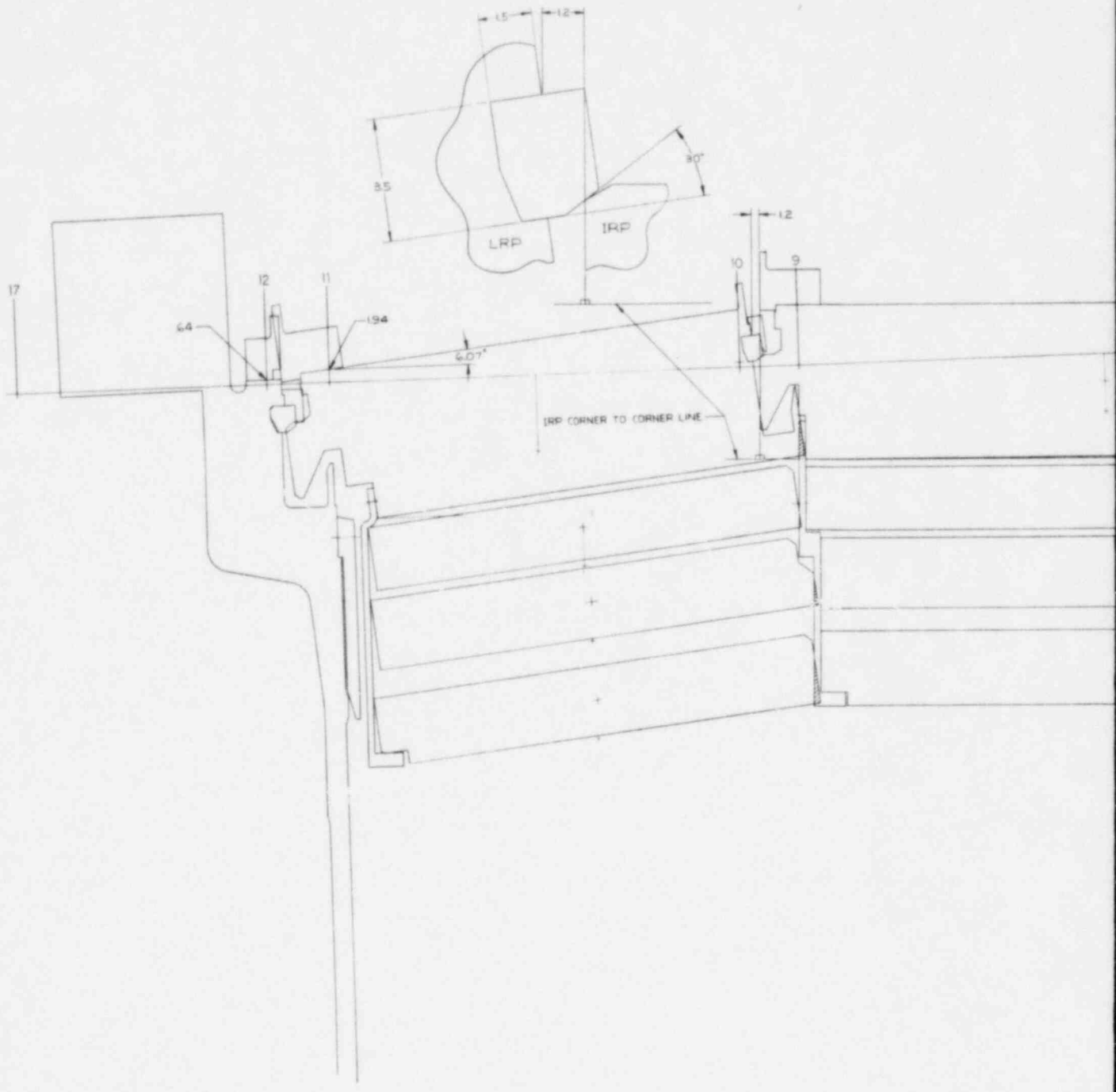
1.5
1.2
3.5
30°
LRP
IRP
1.2
10
9
17
12
11
64
1.94
6.07°
IRP CORNER TO CORNER LINE

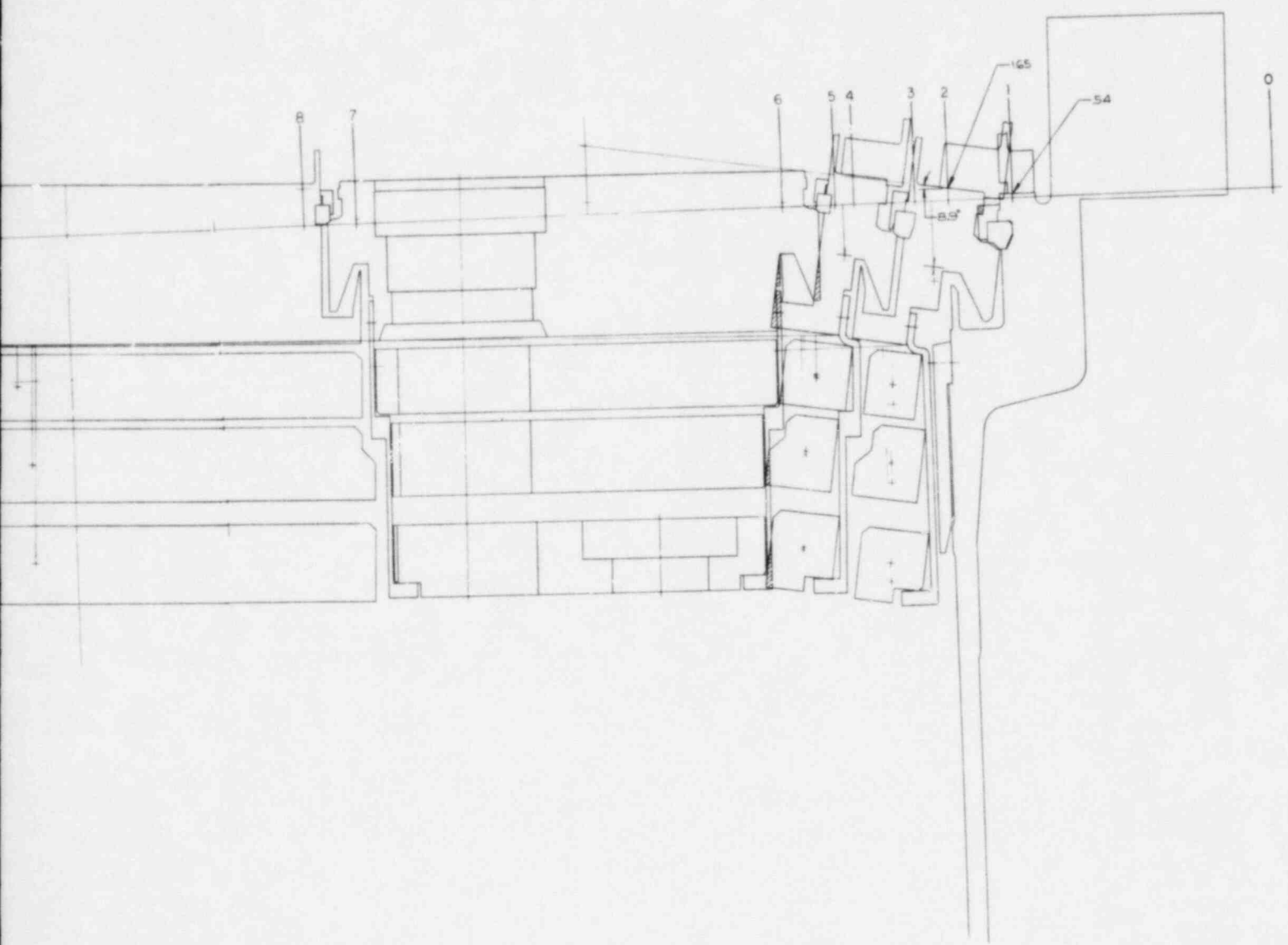

PROJECTED CLOSURE HEAD
DEFLECTIONS AND INTERFERENCES
AT 3000 PSI

FIGURE 8

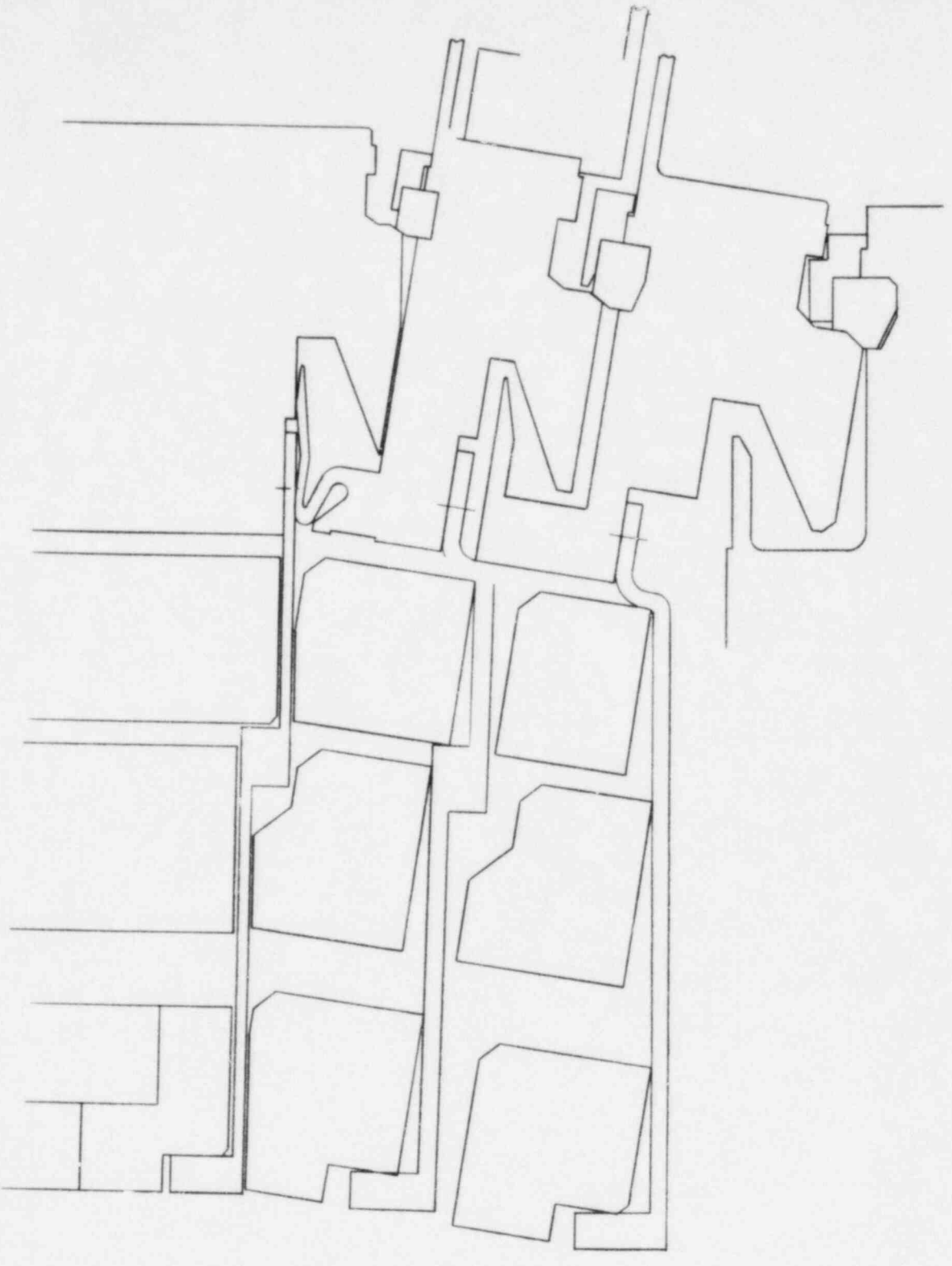

MAXIMUM (3000 PSI) DEFLECTION

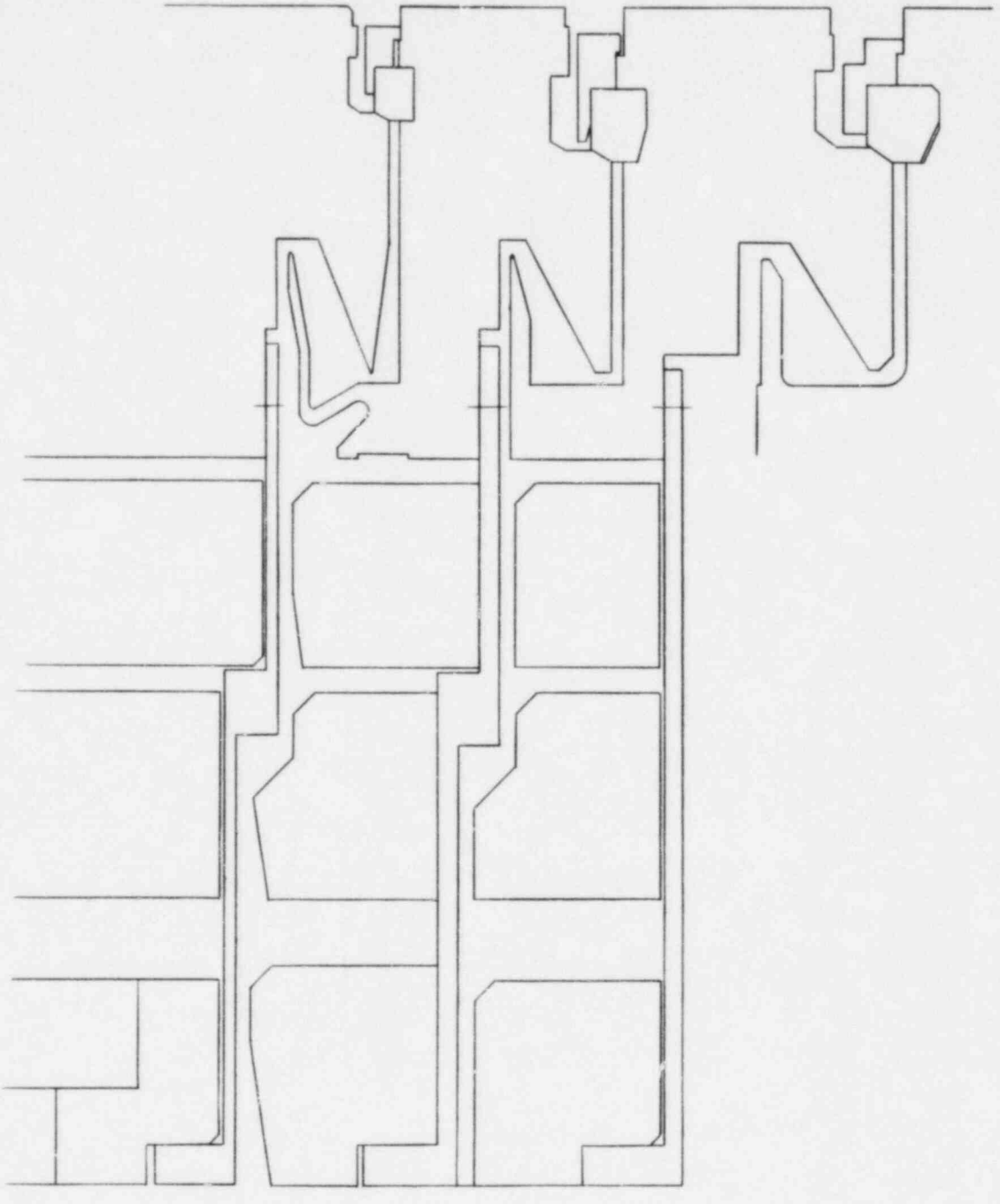

ZERO DEFLECTION

MACHINING MODIFICATIONS PROPOSED
TO ELIMINATE INTERFERENCES AT
THE NODE 5-6 INTERFACE

FIGURE 9

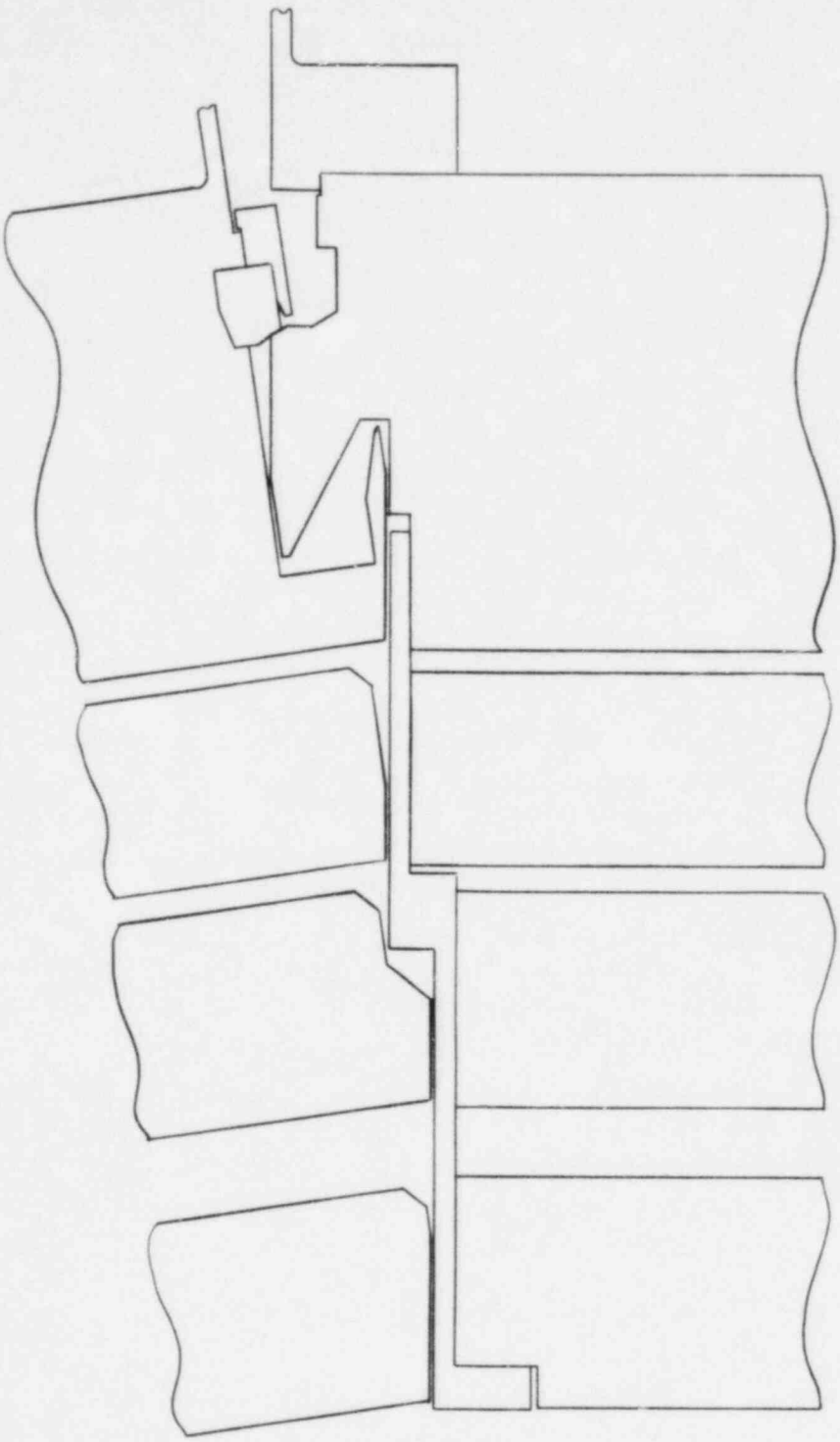

MAXIMUM (3000 PSI) DEFLECTION

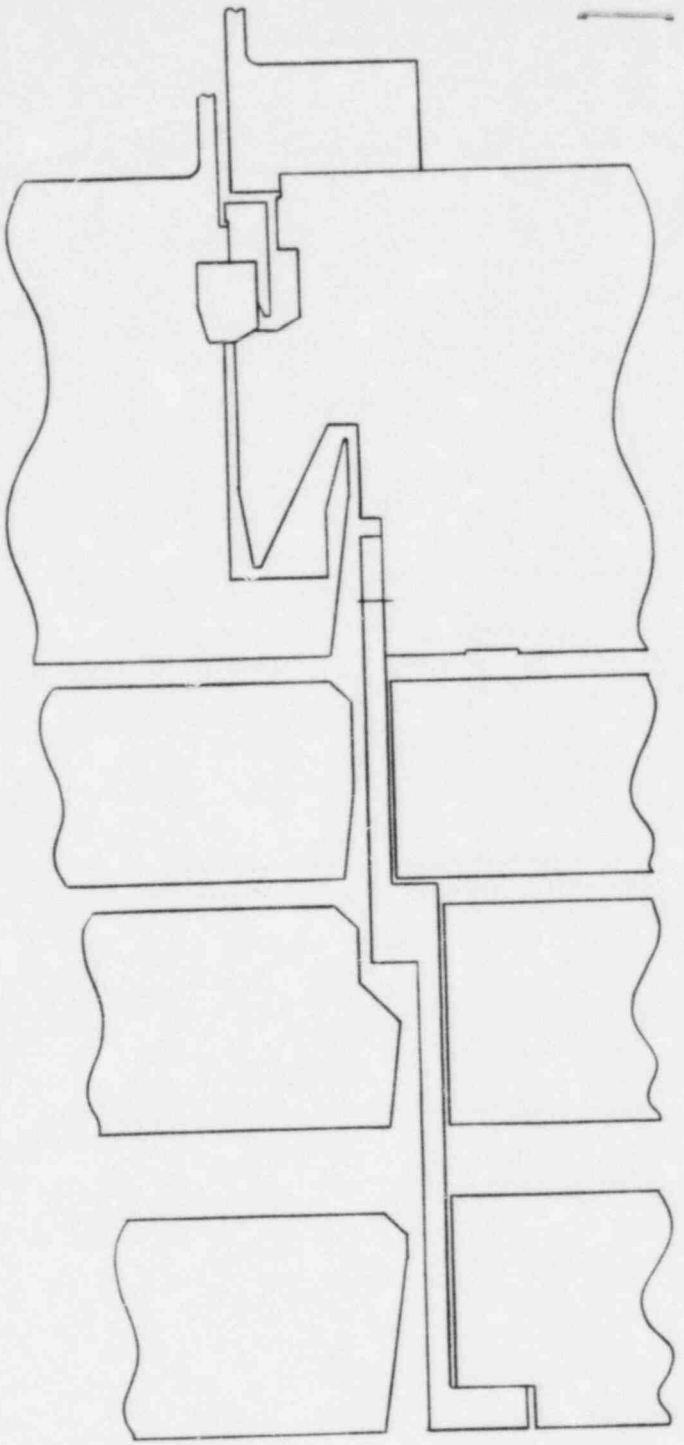

ZERO DEFLECTION

MACHINING MODIFICATIONS PROPOSED TO ELIMINATE INTERFERENCES AT THE NODE 9-10 INTERFACE

FIGURE 10

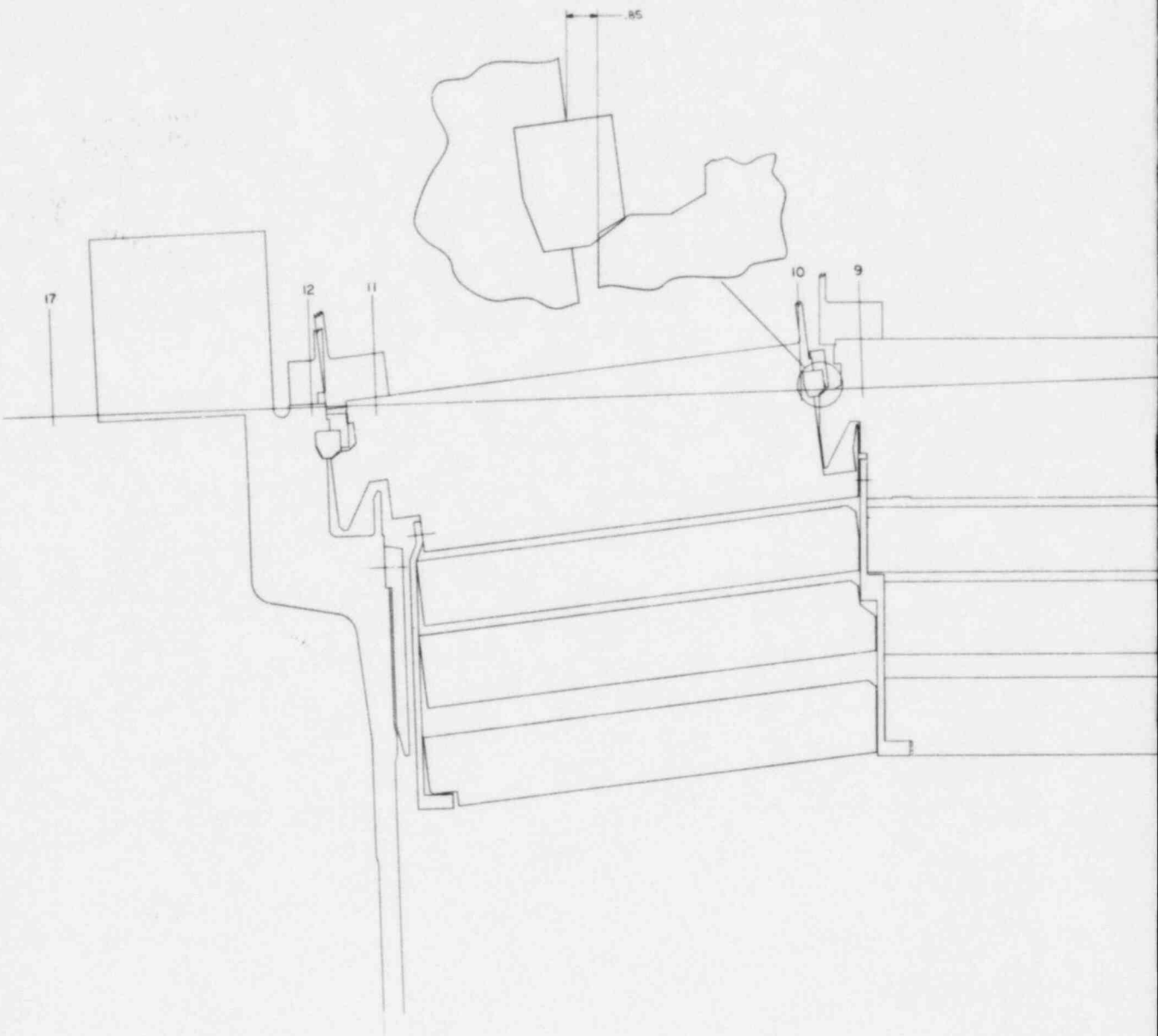
.85
17
12
11
10
9

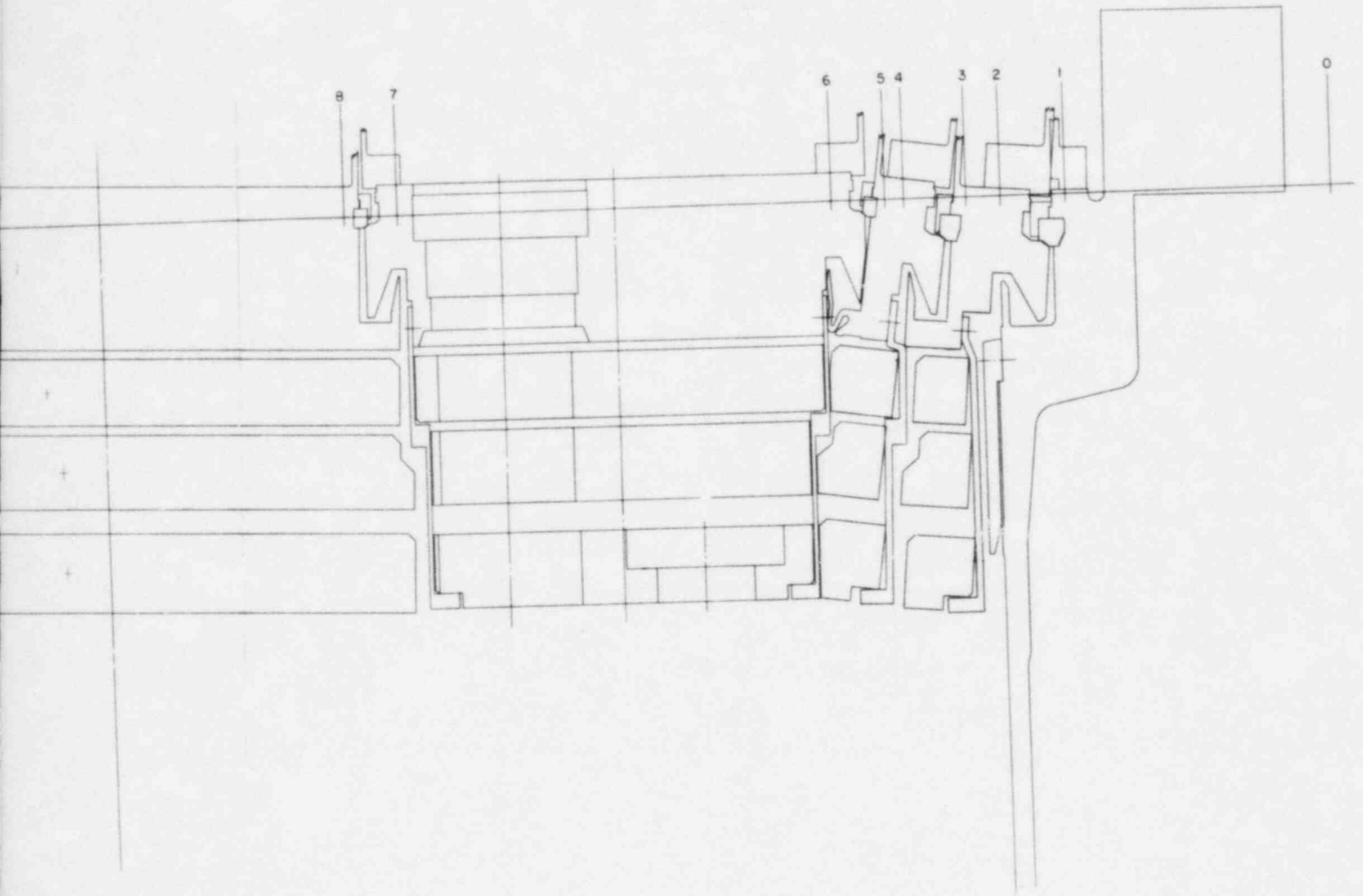

PROJECTED CLOSURE HEAD DEFLECTIONS AT
2700 PSI WITH PROTOTYPE RADIAL RESTRAINT
AT THE LRP-REACTOR VESSEL INTERFACE

FIGURE 11

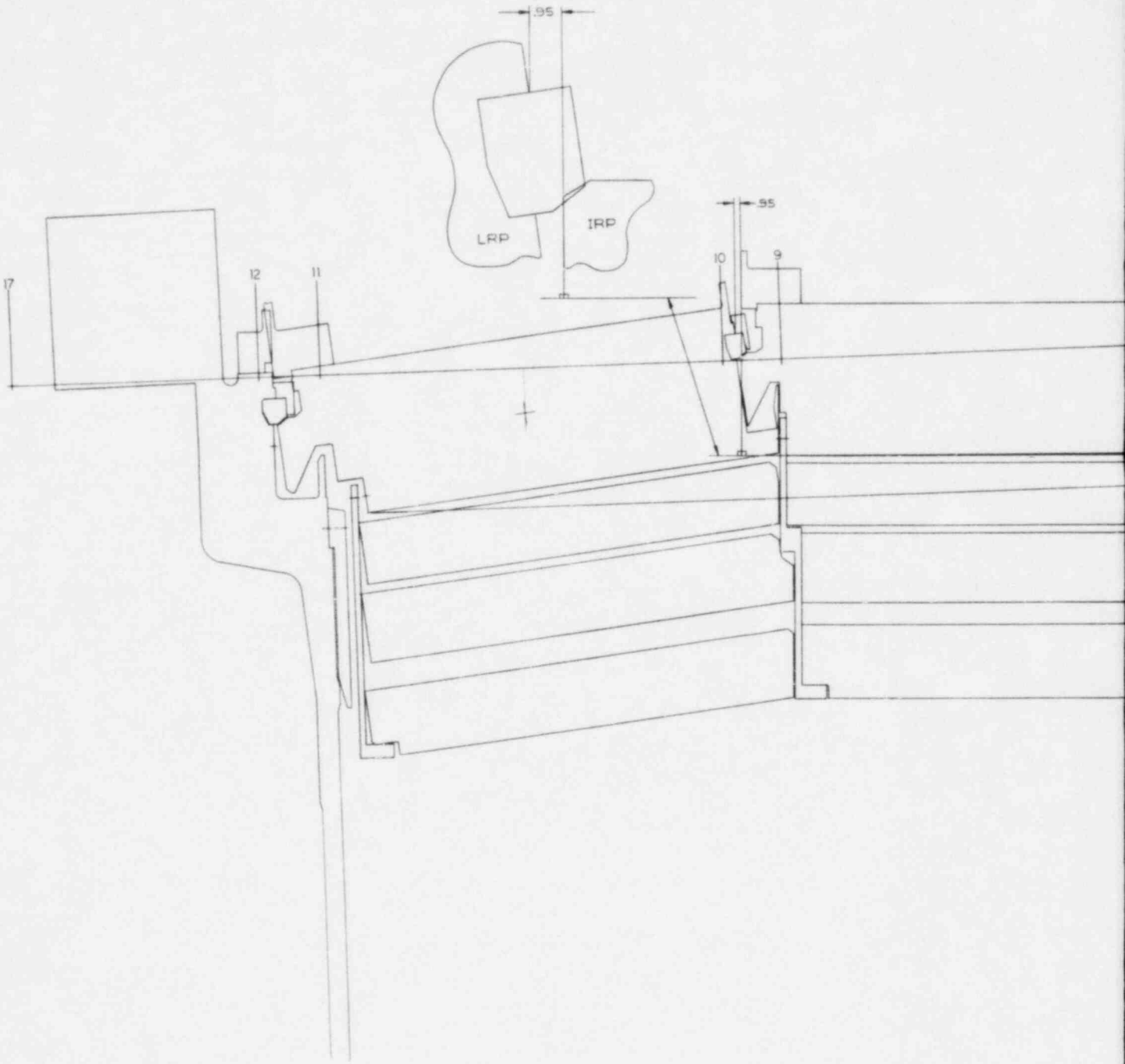
.95
LRP
IRP
.55
17
12
11
10
9

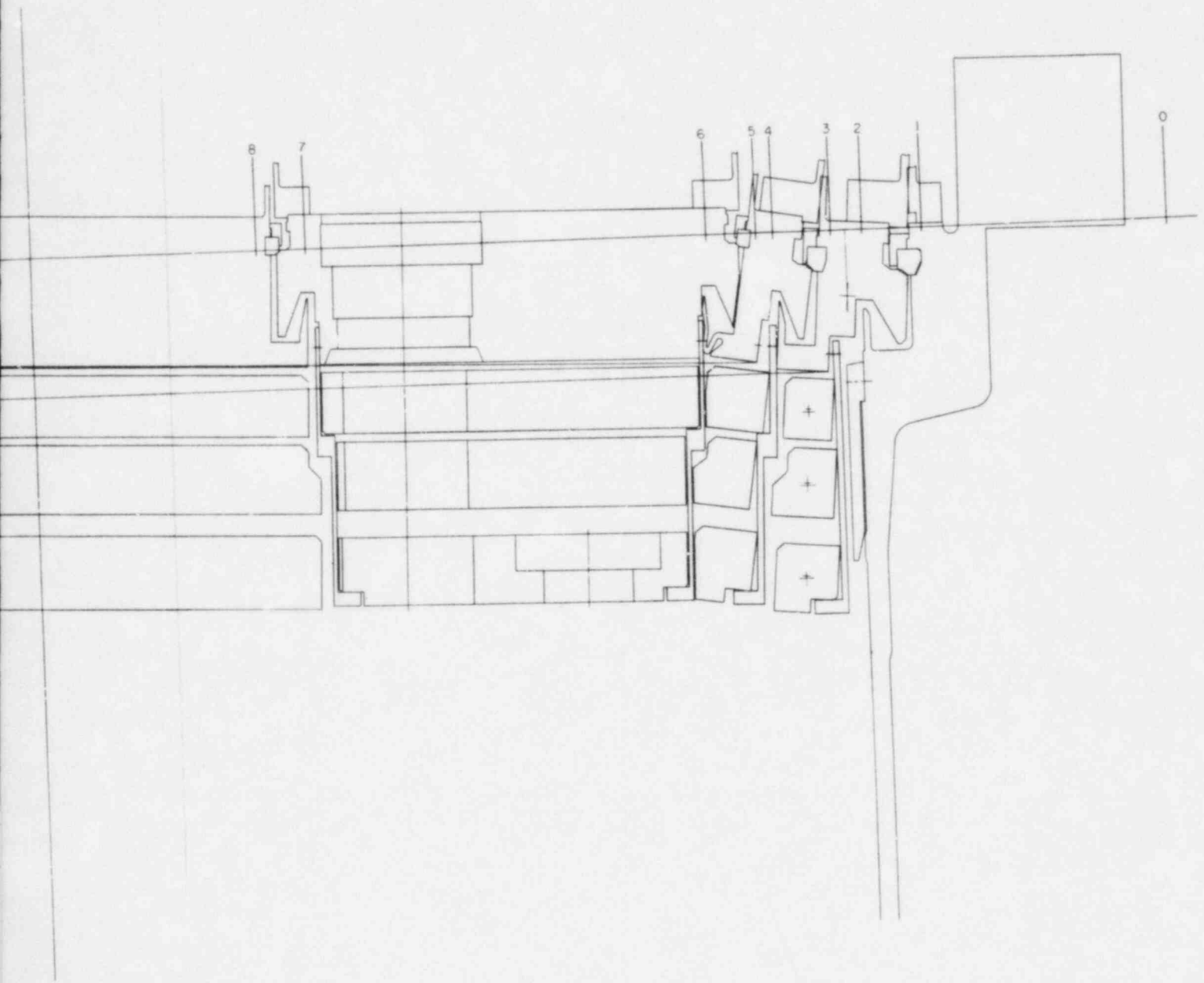

PROJECTED CLOSURE HEAD DEFLECTIONS AT
3000 PSI WITH PROTOTYPE RADIAL RESTRAINT
AT THE LRP-REACTOR VESSEL INTERFACE

FIGURE 12

- The Limiting Load Is Based On Average Shear Stress At 400°F
- Allowable Shear Stress = 0.6 Allowable Tensile Strength
  (ASME Sec. III, B – 3227.2 Pure Shear)
- Allowable Tensile Strength = 0.9 S_u
  0.9 Is A Factor On The Collapse Load Based On The ASME Sec. III
  Appendix F For Faulted Conditions
- Material Data At Critical Region:

COMPONENT	MATERIAL SPEC.	R.T. (1) UTS (KSI)	400°F ESTIMATED UTS (KSI)	DATA SOURCE
R.V. TOP FLANGE	SA-508 C1.2	88.2	78.5	P.O. CCU-239552-B LADISH CO. WE084A
LRP MARGIN RING	SA-540 B-24, C1.1	163.5	153.0	PRIORITY 4 DATA PACKAGE FAG AR-54-7CCN-239588-35
LRP	SA-508 C1.2	83.0	73.87	CHICAGO BRIDGE & IRON DATA PACKAGE P.O. 54-CCW-212567
OUTER RISER BASE FLANGE STUD	SA-540 B-23 C1.1	168.4	160.8	B&W PRIORITY 4 DATA PACKAGE P.O. 54-7CCA-237970

(1) Ultimate Tensile Strength Is The Lowest Of The Test Data Of Each Material

Figure 13
Acceptance Criteria

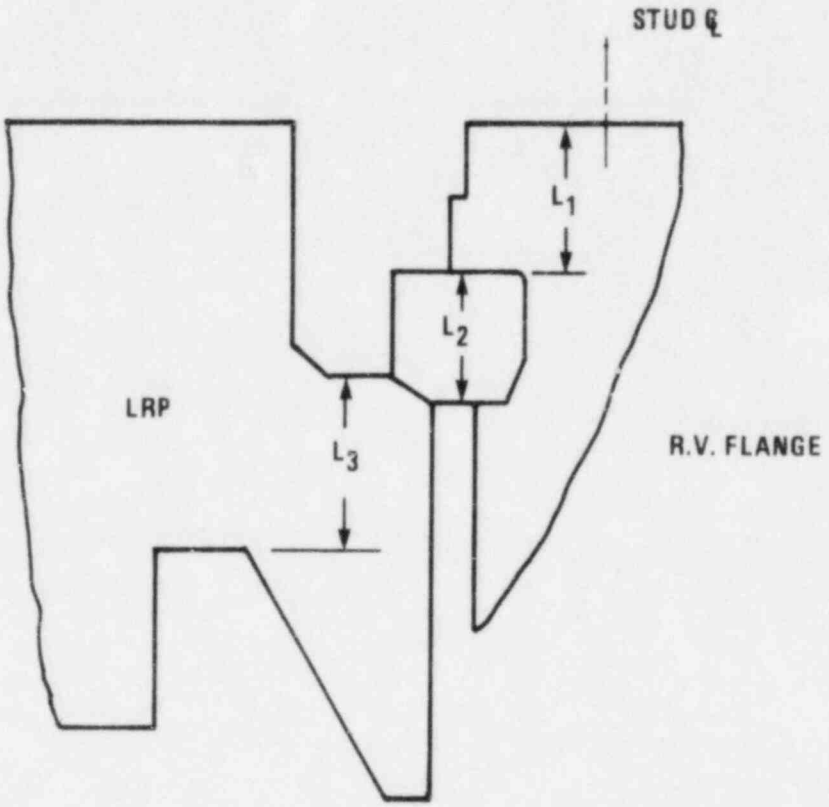

LOCATION	COMPONENT	FORCE (LB/IN CIRC.)	HEIGHT (IN)	AVERAGE SHEAR STR. (PSI)	ALLOWABLE SHEAR STR. (PSI)	ALLOWABLE PRESSURE (PSI)
VESSEL/ TO LRP INTERFACE	R.V. FLANGE	64.25P	L_1 = 3.80	16.91 P	42390	2507
	MARGIN RING		L_2 = 3.50	18.36 P	82620	4500
	LRP		L_3 = 4.60	13.97 P	39890	2855

P = PRESSURE

THE AVERAGE SHEAR STRESSES IN THE INTERMEDIATE AND SMALL SHEAR JOINTS ARE LESS THAN THE ABOVE VALUES.

TOTAL ALLOWABLE PRESSURE = VESSEL FLANGE CAPACITY + FLANGE STUDS CAPACITY
= 2507 + 248 = 2755 PSI

Figure 14
Shear Joint Strength

89 Studs 1.250 – 8 UN – 2A (Shank Area = 1 in^2)

S_w At 400°F = 160800 psi

Allowable Strength = 0.9 S_u = 144720 psi
(0.9 Factor Based On Collapse Load of ASME Sec. III Appendix F)

Total Area = 1 x 89 = 89 in^2

Load Capacity = 144720 x 89 = 1.288×10^7 lbs

Diameter of LRP = 257 in

$$\text{Allowable Pressure} = \frac{1.288 \times 10^7}{\frac{\pi}{4}(257)^2} = 248 \text{ psi}$$

Figure 15
Flange Studs Capacity

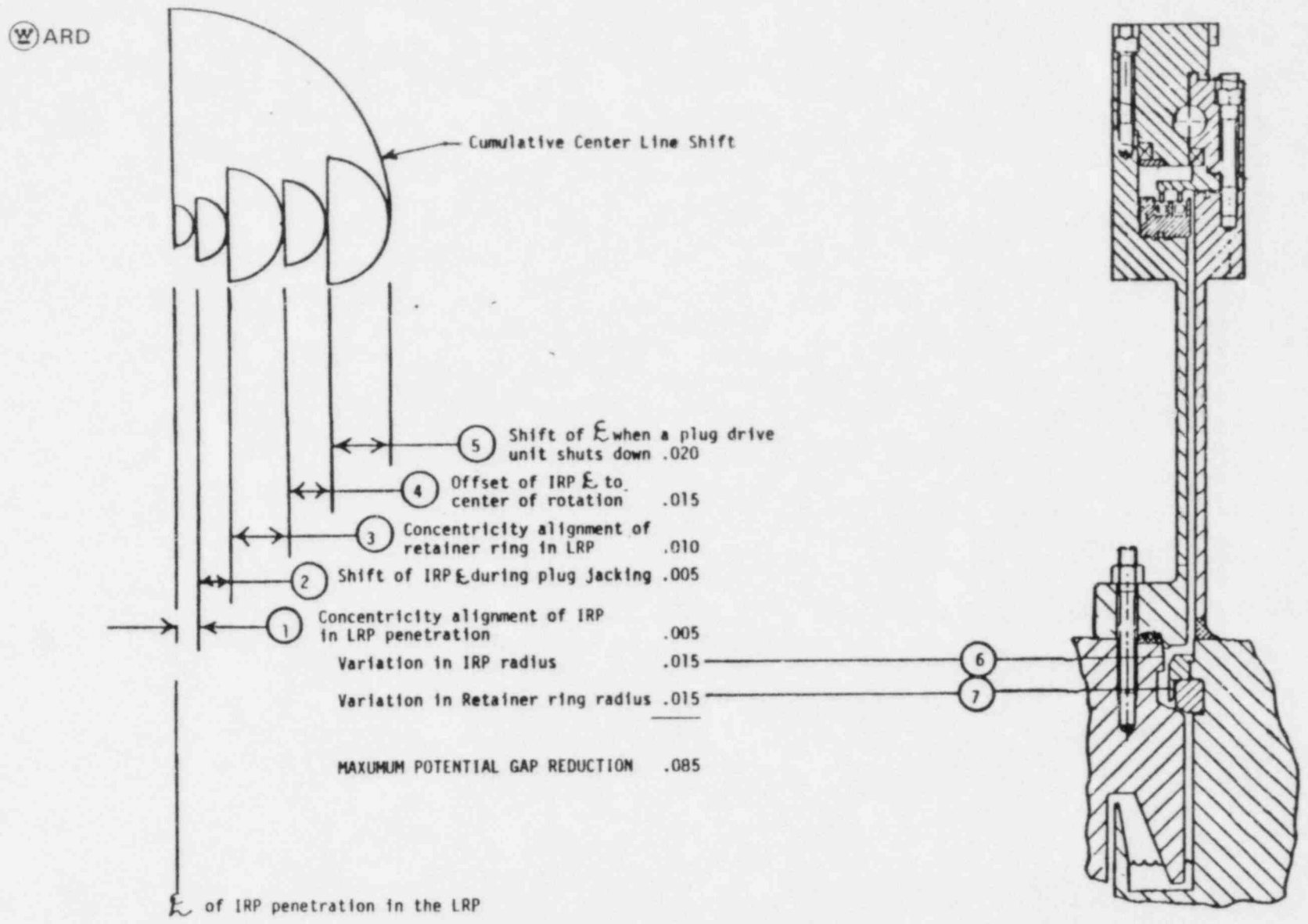

Figure 16
Potential Gap Reduction Factors

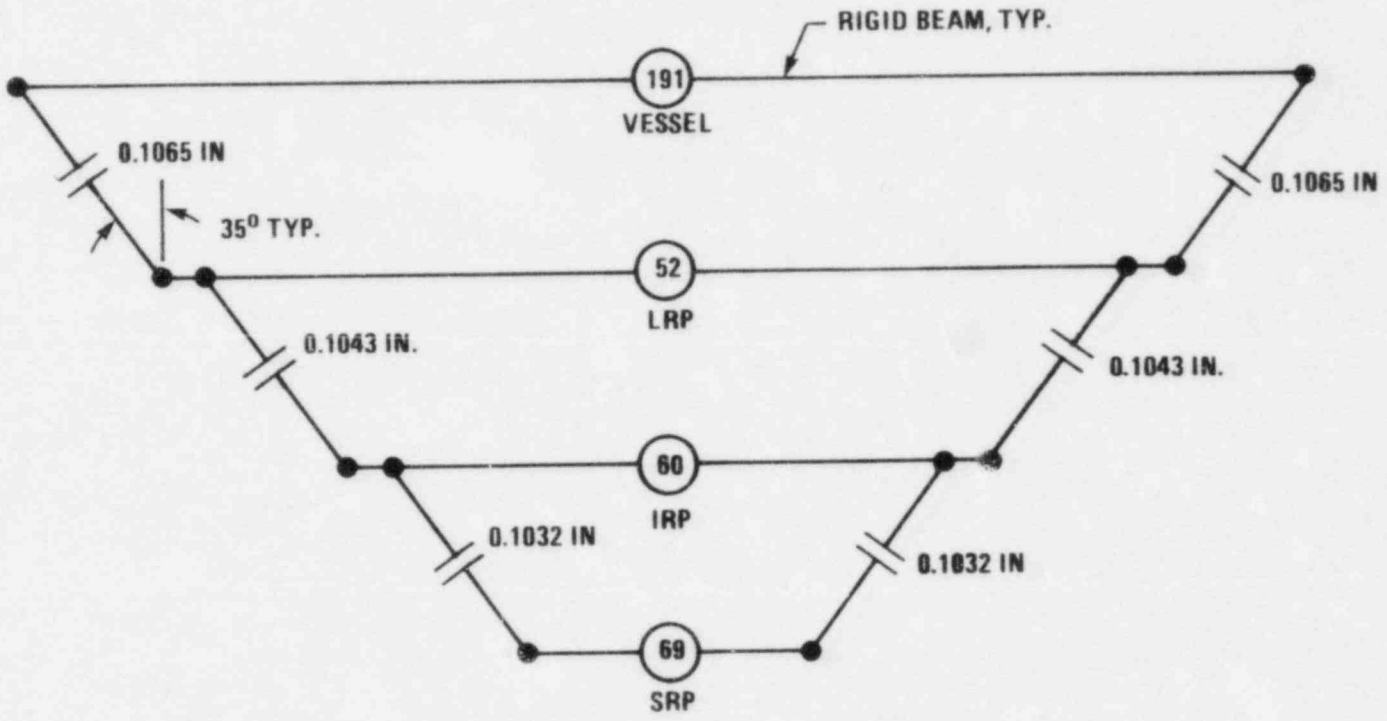

Figure 17
Seismic Model: From SARB No. LRA-SA-78-77

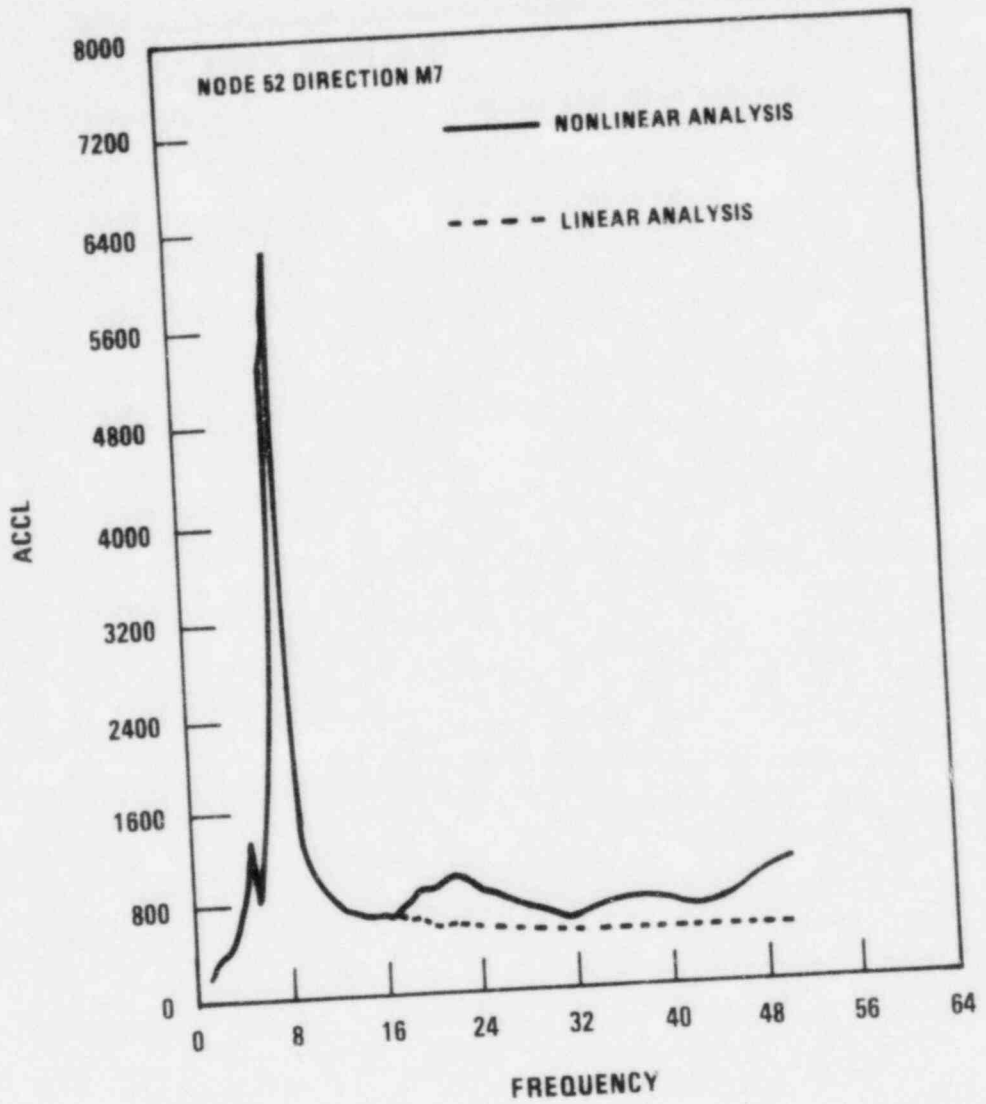

Figure 18
WMTFOBC Vs. WMTFO9C RS at LRP

- Reactor System Seismic Model Is Linear
- Effect Of Inter-Plug Gaps Was Evaluated In A Separate Analysis
- The Results Show That There Is No Significant Difference In The Response Spectra Peaks
- The LRP ZPA Increased, However This Would Be Reduced With Actual Plug Distributed Mass And Stiffness
- It Can Be Concluded That Gap Modification Will Have An Insignificant Effect On The Seismic Response

Figure 19
Head Seismic Response With Reduced Radial Gaps Between Plugs

3000 PSI

1. Plug Primary Strains

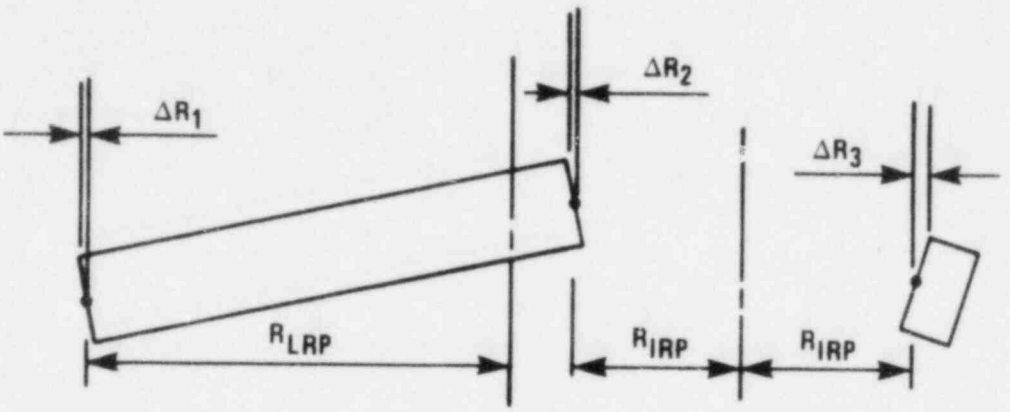

$\epsilon max = \Delta R/R = 1.2\%$ (Uniaxial)

$\epsilon u = 7.0\%$ (SA508 CL 2 At 400°F)

$0.7 \times \epsilon u = 4.9\%$ (0.9 Factor Based On Strain Limit Load Of ASME Section III Appendix F)

2. Attachment Strains

- The LRP O.D. Attachment Is The Most Highly Loaded Attachment
- The LRP O.D. Attachment Geometry Was The Same For The SM 7 And SM 8 Tests
- The Joint Withstood A 2587 PSI Load In The SM 7 Test With No Failures

Figure 20
Plug Strain Summary

M_S = SLUG MASS ($W_S = 0.368 \times 10^6$ LB)

M_H = HEAD MASS ($W_H = 1.046 \times 10^6$ LB)

$M_{H\&S}$ = SLUG MASS + HEAD MASS

V_S = SLUG VELOCITY

$V_{H\&S}$ = VELOCITY OF THE COMBINED SLUG & HEAD MASS

KE_S = SLUG KE AT IMPACT = 75 MJ

$KE_{(H\&S)}$ = ESTIMATE OF THE KE DELIVERED TO THE HEAD

FOR CONSERVATION OF MOMENTUM: -IN AN Inelastic Collision*;

$$V_{M\&S} = V_S \left(\frac{M_S}{M_S + M_H} \right) \quad (1)$$

$$KE_S = \left(\frac{M_S V_S^2}{2} \right) \quad (2)$$

$$KE_{H\&S} = \left(\frac{M_S + M_H}{2} \right) \times V_S^2 \left(\frac{M_S}{M_S + M_H} \right)^2$$

$$KE_{H\&S} = \frac{V_S^2 M_S^2}{2(M_S + M_H)} = KE_S \left(\frac{M_S}{M_S + M_H} \right) \quad (3)$$

$$KE_{H\&S} = \frac{75 \times 0.368}{(1.046 + 0.368)} = 19.5 \text{ MJ}$$

$$KE_{H\&S} = 19.5 \times 8.85 \times 10^6 = 173 \times 10^6 \text{ LB.IN.}$$

*See Appendix A for an evaluation of the appropriateness of using this inelastic collision model.

Figure 21
Head Energy Input

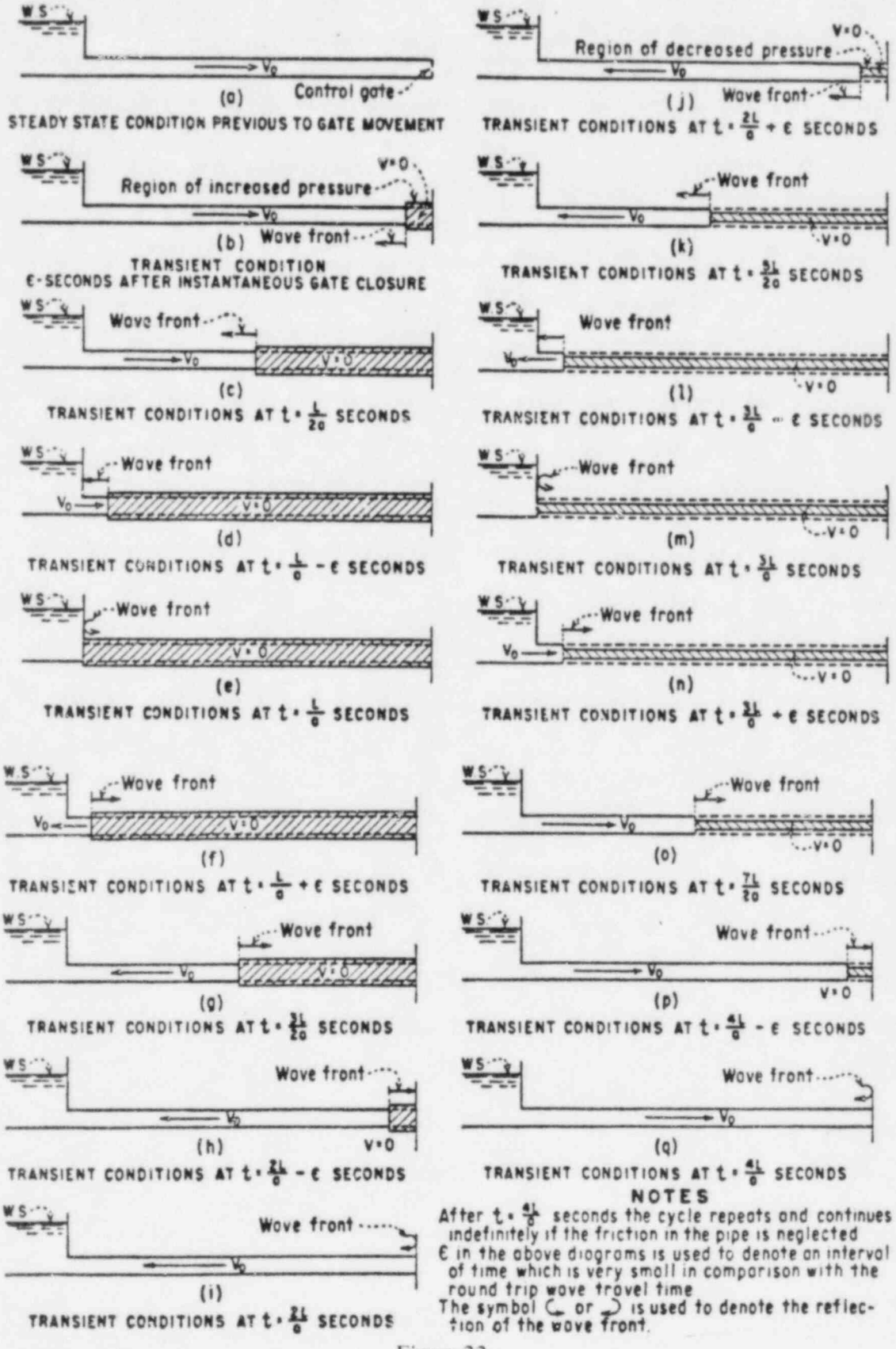

Figure 22

Propagation of Pressure Waves Caused by an Instantaneous Complete Gate Closure

1. DATA

SLUG WEIGHT = 0.368×10^6 lb

SLUG TEMPERATURE ≈ 1000°F

SLUG DENSITY = 51 lb/ft^3 = 0.029 lb/in^3

SODIUM COMPRESSIBILITY = $0.29/GP_a$ (SMH)

1 $GP_a = 0.145 \times 10^6$ lb/in^2

MAXIMUM INTERFACE PRESSURE AT IMPACT = 5300 PSI

2. ENERGY CONTENT ESTIMATE

THE "WATERHAMMER" PRESSURE THROUGHOUT THE LENGTH OF THE SLUG AT TIME $t = \frac{L}{a}$ SECONDS AFTER THE IMPACT WILL BE A UNIFORM 5300 PSI (Reference WATERHAMMER ANALYSIS, John Parmakian)

$$\text{COMPRESSION ENERGY STORED} = \frac{\Delta . P}{2}$$

$$PEs = \frac{V . P^2}{2K}$$

$$K = \text{BULK MODULUS} = \frac{0.145 \times 10^6}{0.29} = 0.5 \times 10^6 \text{ lb/in}^2$$

$$\text{VOLUME} = \frac{0.368 \times 10^6 \times 12^3}{51} = 12.5 \times 10^6 \text{ in}^3$$

$$\therefore PEs = \frac{12.5 \times 10^6 \times 5300^2}{2 \times 0.5 \times 10^6} = 351 \times 10^6 \text{ lb.in}$$

$$1 \text{ MJ} = 8.85 \times 10^6 \text{ lb.in}$$

$$\therefore PEs = \frac{351 \times 10^6}{8.85 \times 10^6} = 39.6 \text{ MJ}$$

Figure 23
Slug Bulk Compression Energy

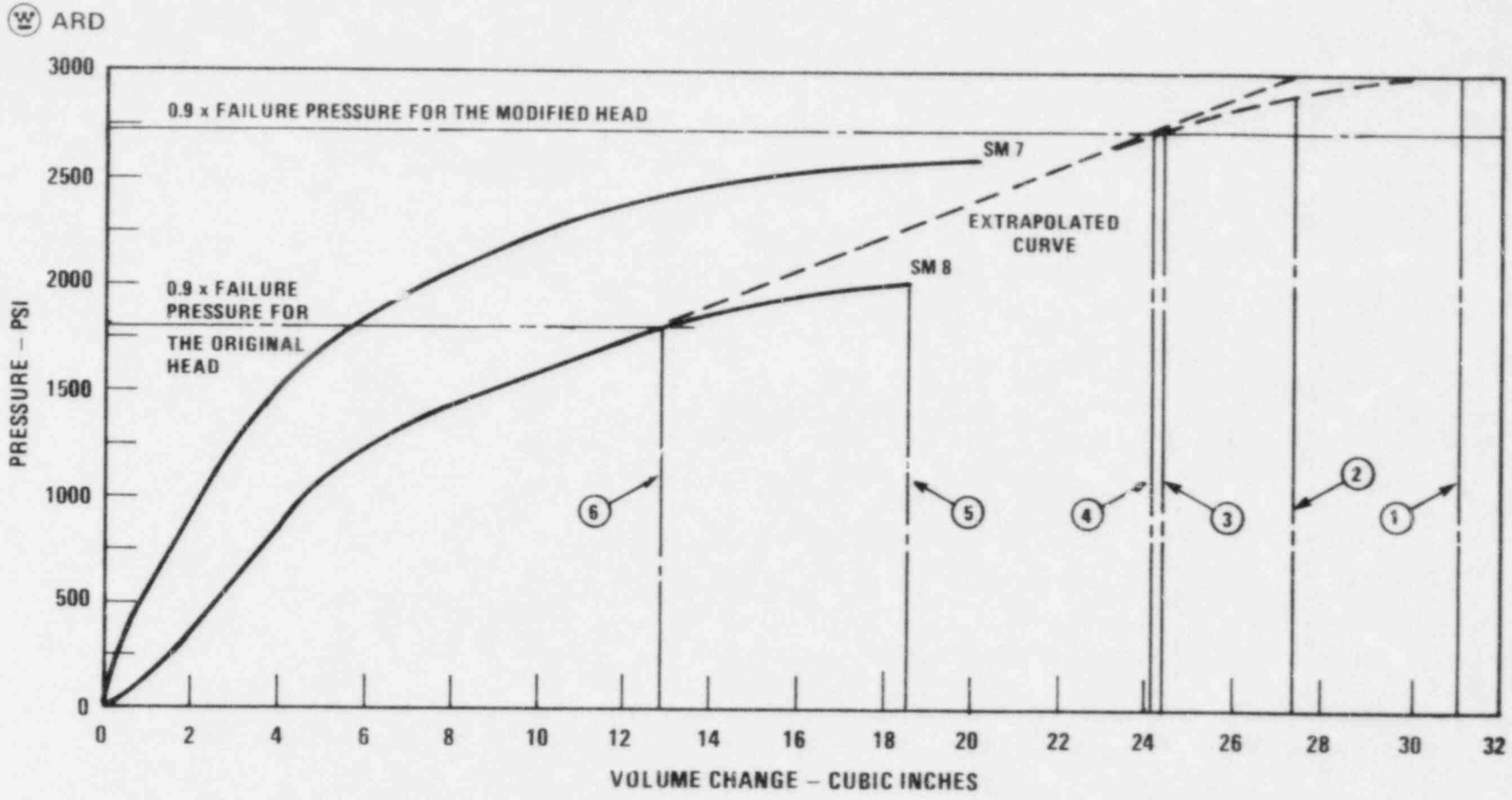

Figure 24
Pressure-Volume Change for Original & Modified Head Designs

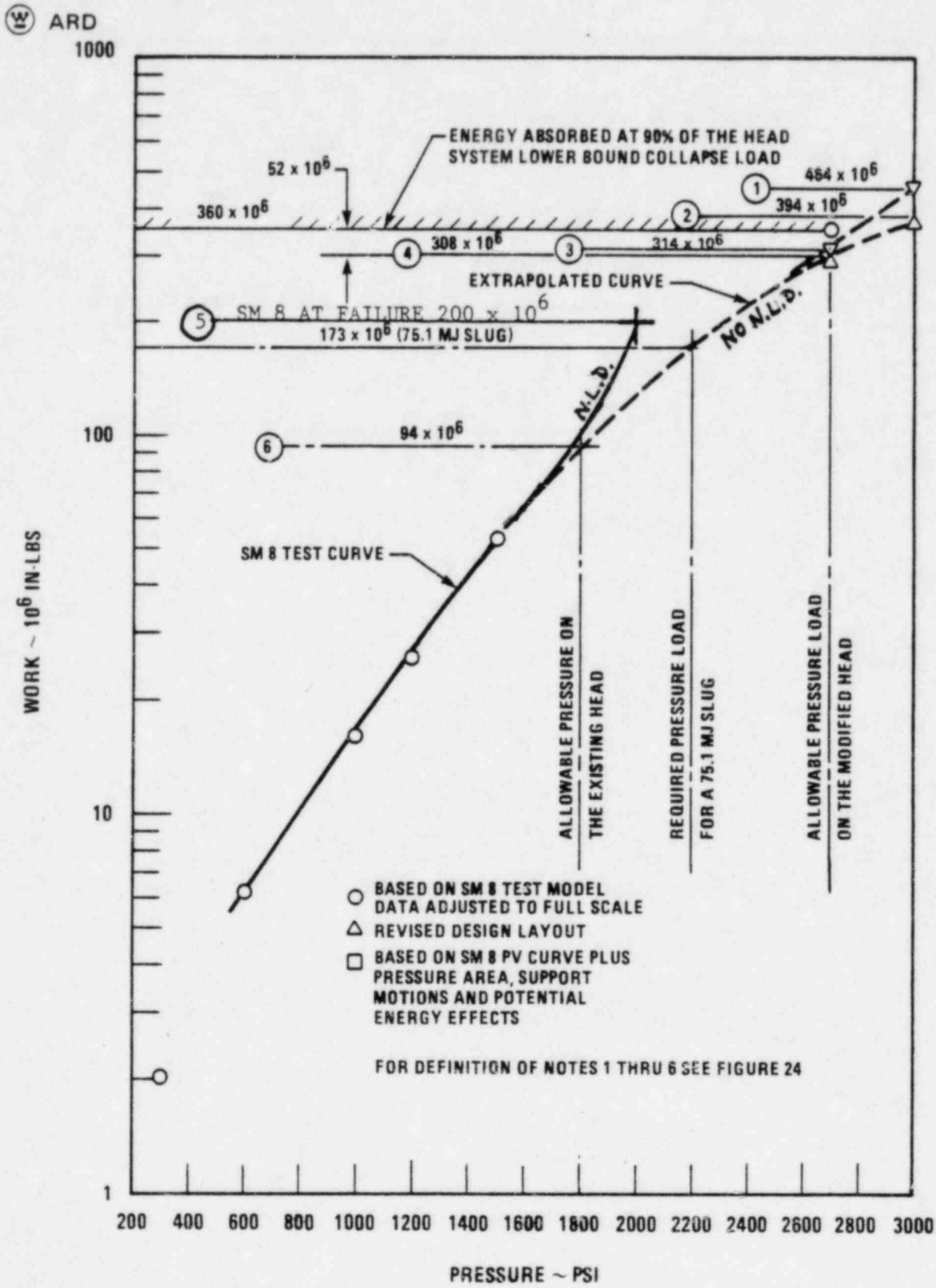

Figure 25
Head System Energy Absorbtion Capability

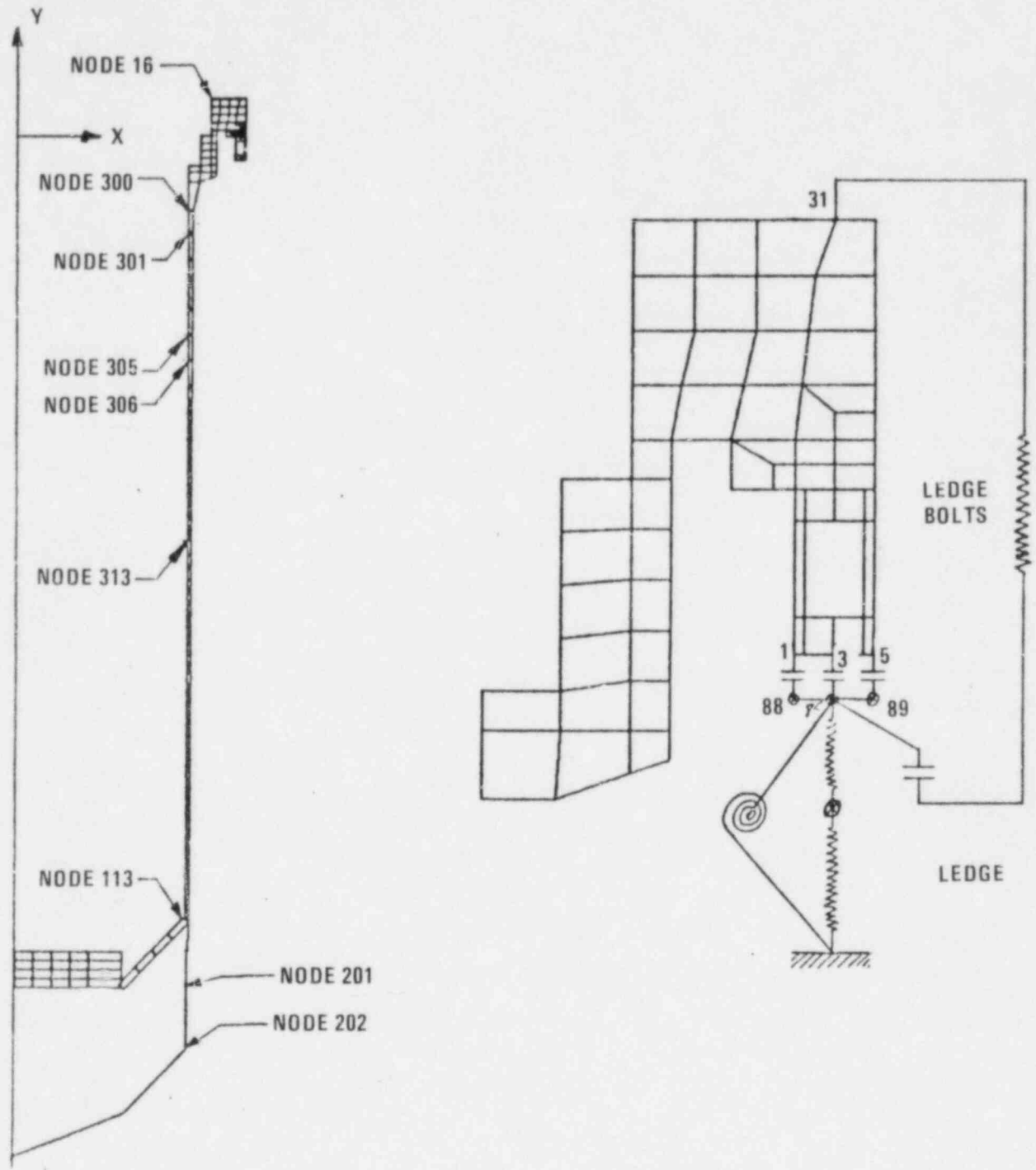

Figure 26
SMBDB Analysis Model

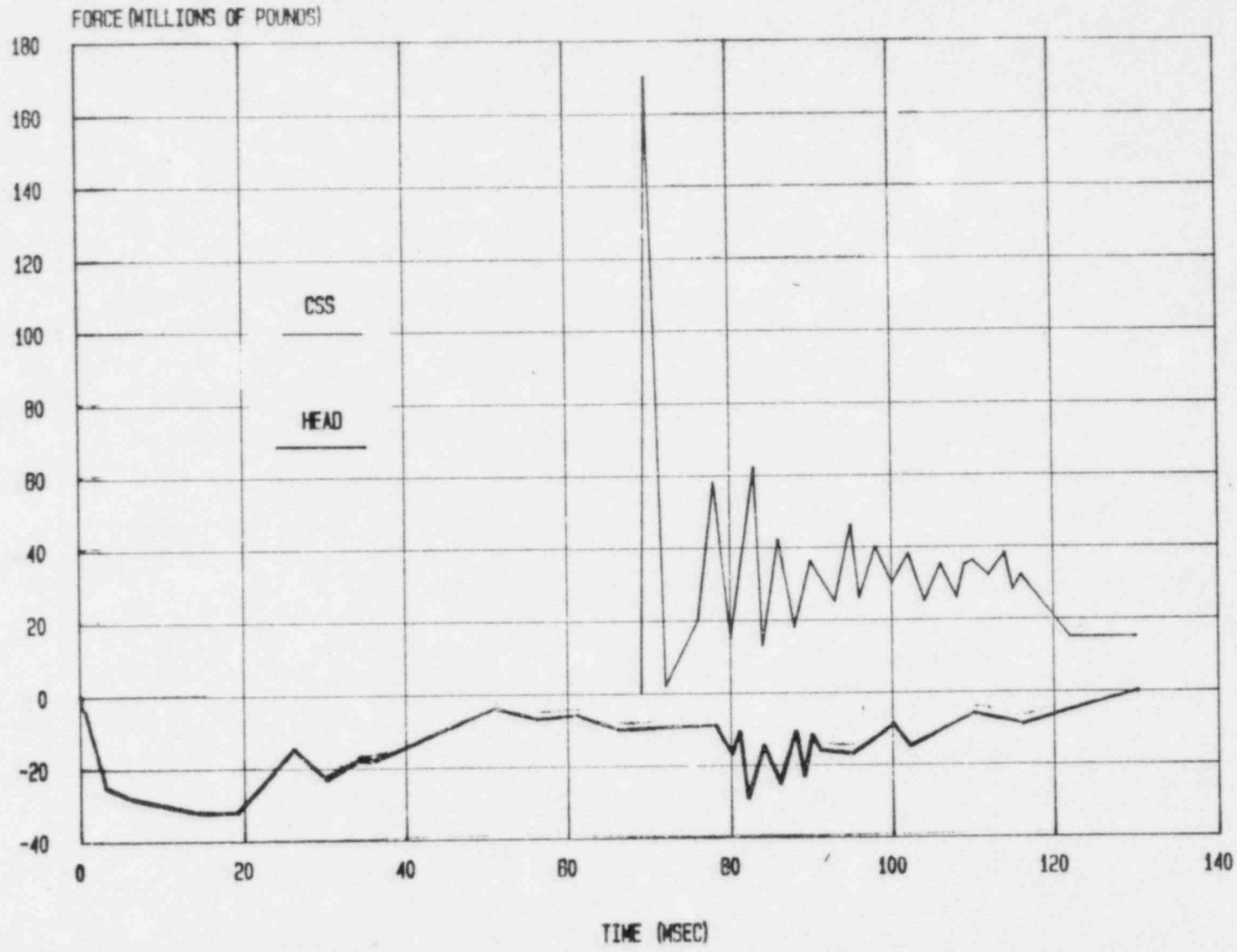

Figure 27
Force Time History
Head Up/Force CSS Down/Force

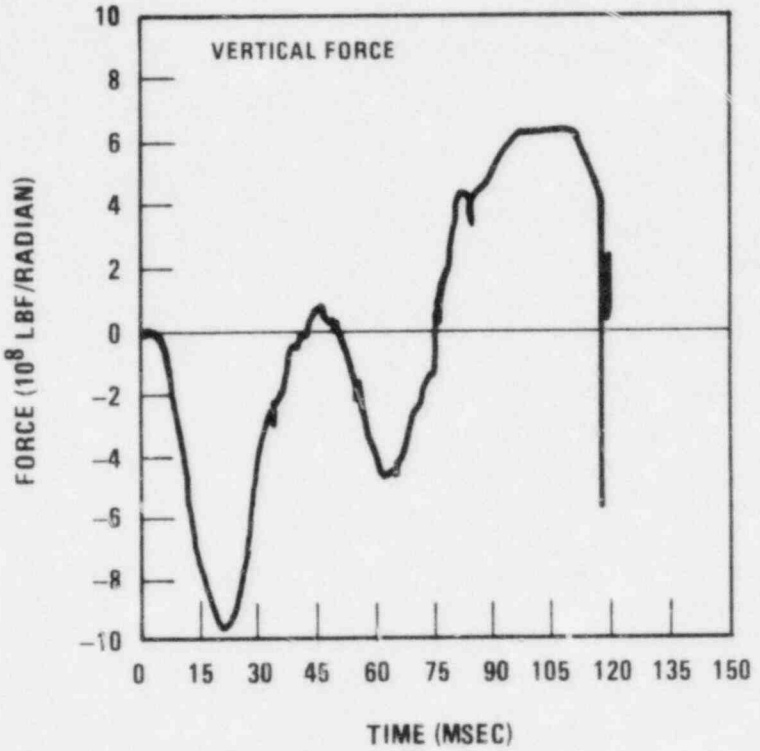

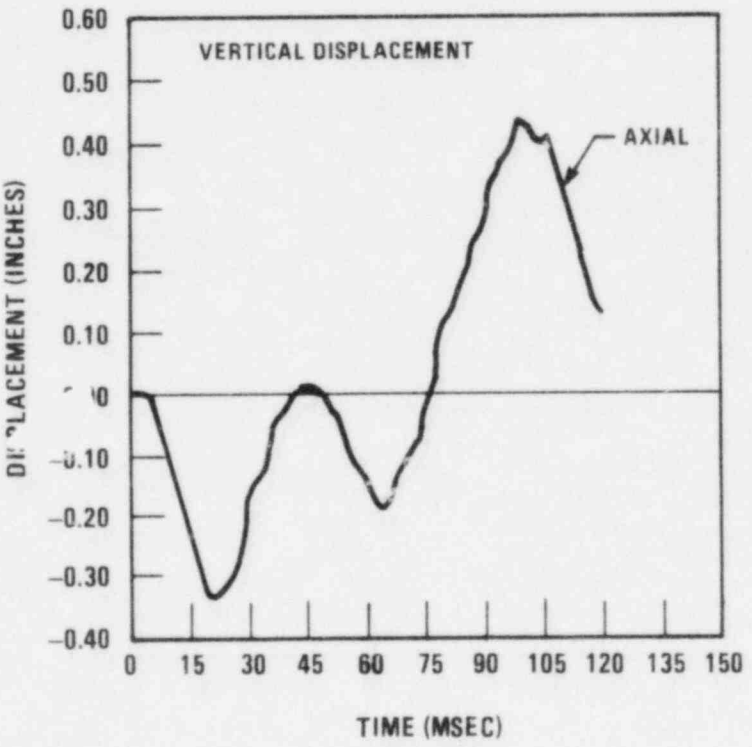

Figure 28
Vessel Flange SMBDB Response

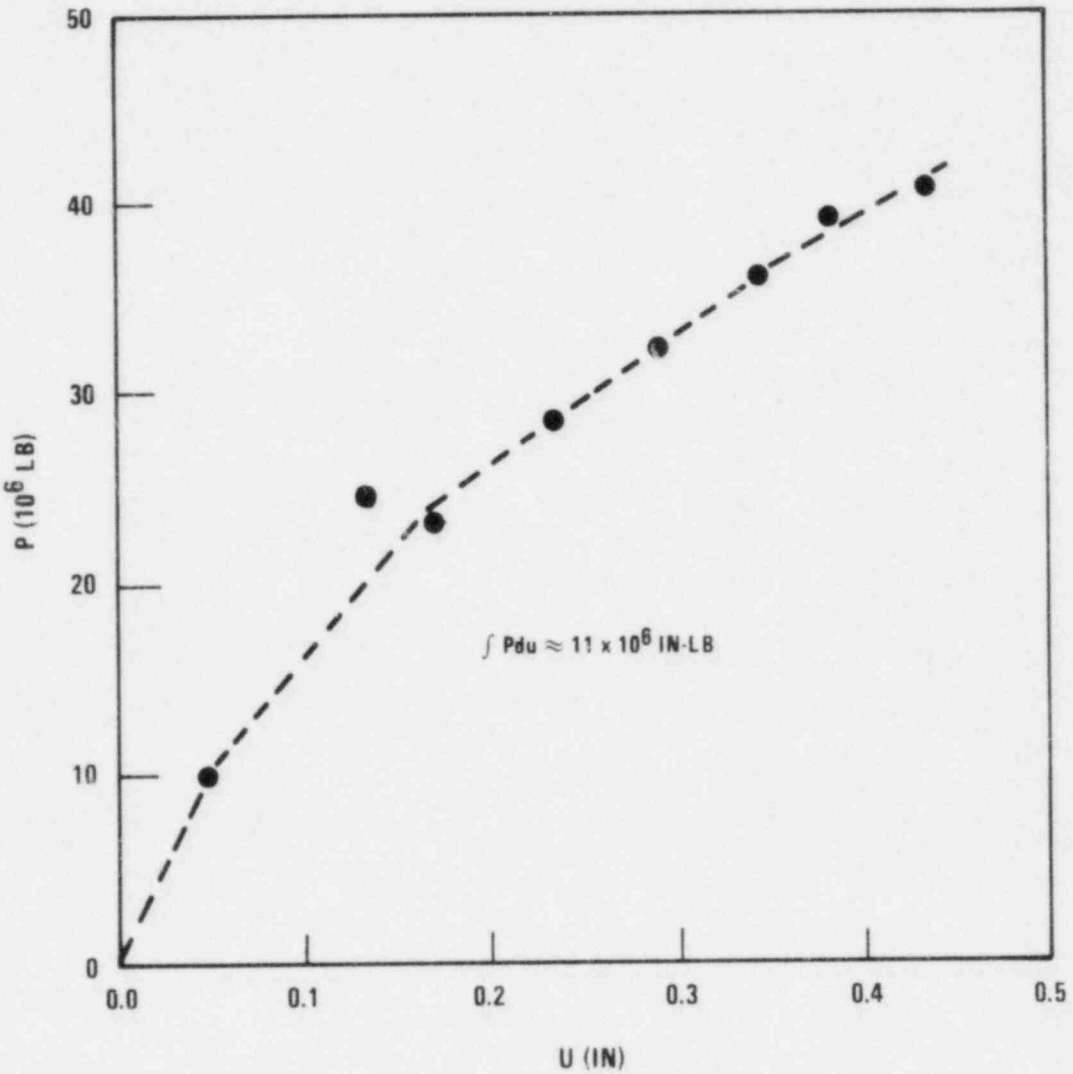

Figure 29
Reactor Vessel Support & Ledge Dynamic Force-Deflection Relationship (75 MJ Slug Load)

HEAD CONFIGURATION	LOADING CONDITION	HEAD PRESSURE PSI	ENERGY ABSORBTION FROM THE EXTRAPOLATED TEST P-V CURVE LB-IN	ADDITIONAL HEAD SYSTEM ENERGY CAPACITY (1) LB-IN	TOTAL HEAD SYSTEM ENERGY CAPACITY LB-IN
EXISTING HEAD	COLLAPSE LOAD	2010	130×10^6	~	~
EXISTING HEAD	90% COLLAPSE LOAD	1800	94×10^6	~	$\geq 94 \times 10^6$
MODIFIED HEAD (2)	COLLAPSE LOAD	3000	394×10^6	~	~
MODIFIED HEAD (2)	90% COLLAPSE LOAD	2700	308×10^6	$\geq 52 \times 10^6$ (2)	360×10^6

THE MODIFIED HEAD ENERGY ABSORBTION CAPABILITY
CORRESPONDS TO A SLUG ENERGY OF 156 MJ

NOTES:
1. THE ADDITIONAL HEAD SYSTEM ENERGY ABSORBTION CAPACITY DERIVES FROM (a) HEAD SYSTEM POTENTIAL ENERGY (b) HEAD SUPPORT SYSTEM STRAIN ENERGY AND (c) ADJUSTMENTS TO ACCOUNT A SMALL NON PROTOTYPIC REPRESENTATION OF THE HEAD PRESSURE AREA IN THE SM 8 MODEL
2. THE ADDITIONAL HEAD SYSTEM ENERGY ABSORBTION CAPACITY WAS ESTIMATED FOR THE MODIFIED HEAD ONLY. SMALLER VALUES WOULD APPLY TO THE EXISTING HEAD DESIGN

Figure 30
Closure Head System Energy Absorbtion Summary

DEFINITION OF CONFIRMATORY TEST PROGRAM

The ability of the closure head structure to remain integral following the SMBDB loads will be confirmed using static and dynamic tests. These tests are outlined below.

1. Static Test (SM-9)

1.1 Objective

To define the head deflection as a function of pressure up to the failure point for a prototypic configuration consisting of the head (including proposed modifications), the risers and the underhead shielding. Confirm the expected failure mode with the proposed modifications.

1.2 Test Description

A 1/20th scale model configuration will be tested using procedures and instrumentation analogous to the SM-7 and SM-8 tests. To the extent practical, the configuration will be tested to the point of complete disengagement of a plug.

1.3 Information To Be Obtained and Its Use

The pressure-deflection information will be compared to that from the SM-8 test to assess the increase in capability as a result of the proposed design modifications and the inclusion of the risers. The head capability will be estimated for this configuration. This information will be factored into a decision on modifying the head and will assist in planning the dynamic test SM-10.

1.4 Schedule

This test is expected to be run when the final design is established and prior to finalizing plans for SM-10.

2. Dynamic Test (SM-10)

2.1 Objectives

A. To confirm that the closure head structure would remain integral following the SMBDB loads by accurately simulating the loads and the structures in a dynamic scale model test.

B. To provide dynamic data from the head for use in assessing the response of head mounted components to the SMBDB loads.

C. To provide sufficient information on deflections and deformations to permit an assessment of sodium leakage in the prototypic case.

2.2 Test Description

A 1/20th scale model configuration of the reactor vessel, head and internals will be tested in a dynamic test analogous to SM-5 with the following significant differences:

A. The head will be modified to reflect any design changes.

B. The risers will be included.

C. The Upper Internals Structure will be deleted (this will provide a good simulation of the dynamic loads that have been used as SMBDB requirements using an experimental charge similar to that in SM-5).

2.3 Information To Be Obtained and Its Use

Instrumentation will generally be similar to that in SM-5, with possible additional instrumentation to achieve objectives B. and C.

Objective A will have been achieved if the head plugs remain integral at the conclusion of the test.

Objectives B. and C. will have been achieved if the required parameters are measured successfully. Those parameters will be used in assessments of the response of head mounted components and sodium leakage. Those assessments, in turn, will be used to confirm the integrity of the RCB following any sodium releases that may be predicted.

2.4 Schedule

The schedule objective for this test will be completion during 1984.

FEASIBILITY OF ACCOMMODATING LARGE RELEASES OF SODIUM THROUGH THE CLOSURE HEAD

The Reactor Containment Building (RCB) is capable of accommodating large releases of sodium through the reactor vessel closure head without failing. Table 3-10 in CRBRP-3, Volume 2 provides the estimated pressure capability as a function of temperature. For steel shell temperatures up to several hundred degrees Fahrenheit, the pressure capability is in excess of 40 psig. Even at a steel shell temperature as high as 700°F, the pressure capability is in excess of 30 psig.

Information on the consequences of large releases of sodium to the RCB was provided to NRC in a meeting on April 27, 1982. This enclosure provides the results of parametric studies presented in that meeting. The analyses focus on two types of assumed releases. In both types, the release is assumed to be from the closure head in the form of a sodium spray. One type of release is assumed to a spray high into the containment atmosphere (100 ft.). This simulates an unimpeded release into the RCB. The second type of release is assumed to be a spray within the head access area (14 ft.). This simulates a condition in which the spray is deflected by existing or additional hardware so that it remains within the confines of the head access area. However, the head access area is not assumed to be a closed volume; rather, it is in communication (from the pressure standpoint) with the RCB. The results of these studies (Figures 1-7) can be summarized as follows:

1. Even assuming a spray release high into the containment, a release in excess of 40,000 pounds of sodium would be required to approach a containment pressure of 30 psig (Figure 2).

2. If spray releases of that magnitude ($\sim$ 40,000 pounds) are restricted to the height of the head access area, the resulting containment pressure would only be $\sim$ 6 psig (Figure 2).

3. Because of the small and decreasing slope of the pressure vs. sodium release curve, when the release is restricted to the head access area (Figure 2), it is apparent that even releases of hundreds of thousands of pounds of sodium would not challenge the containment integrity.

4. The containment steel shell temperatures would remain well below 200°F for a release of 40,000 pounds of sodium into the upper containment and would remain below 100°F for similar quantities restricted to the head access area (Figure 7). These temperature calculations are conservative since they represent the equilibration temperature of the atmosphere and steel shell, neglecting any heat transfer from the steel shell.

Based on these results, the following conclusions have been reached:

1. Even if sodium is sprayed into the upper containment, the design can accommodate tens of thousands of pounds of sodium spray.

2. If the sodium spray is restricted to the head access area, either through consideration of existing features or the provision of additional features, the containment design could accommodate hundreds of thousands of pounds of sodium spray.

To place these quantities of sodium in perspective, the total quantity of sodium in the reactor vessel above the top of the core barrel is approximately 300,000 pounds.

SCOPE OF PARAMETRIC STUDIES

- CONTAINMENT PRESSURE VS. SODIUM RELEASE FOR INSTANTANEOUS COMBUSTION BOUNDING ASSUMPTION
- SPRAY CODE CALCULATIONS FOR LARGE RELEASES INTO THE RCB
- SPRAY CODE CALCULATIONS FOR LARGE RELEASES INTO THE HEAD ACCESS AREA
- SENSITIVITY TO SODIUM TEMPERATURE
- SENSITIVITY TO DROPLET DIAMETER
- SENSITIVITY TO SPRAY DURATION FOR FIXED QUANTITY

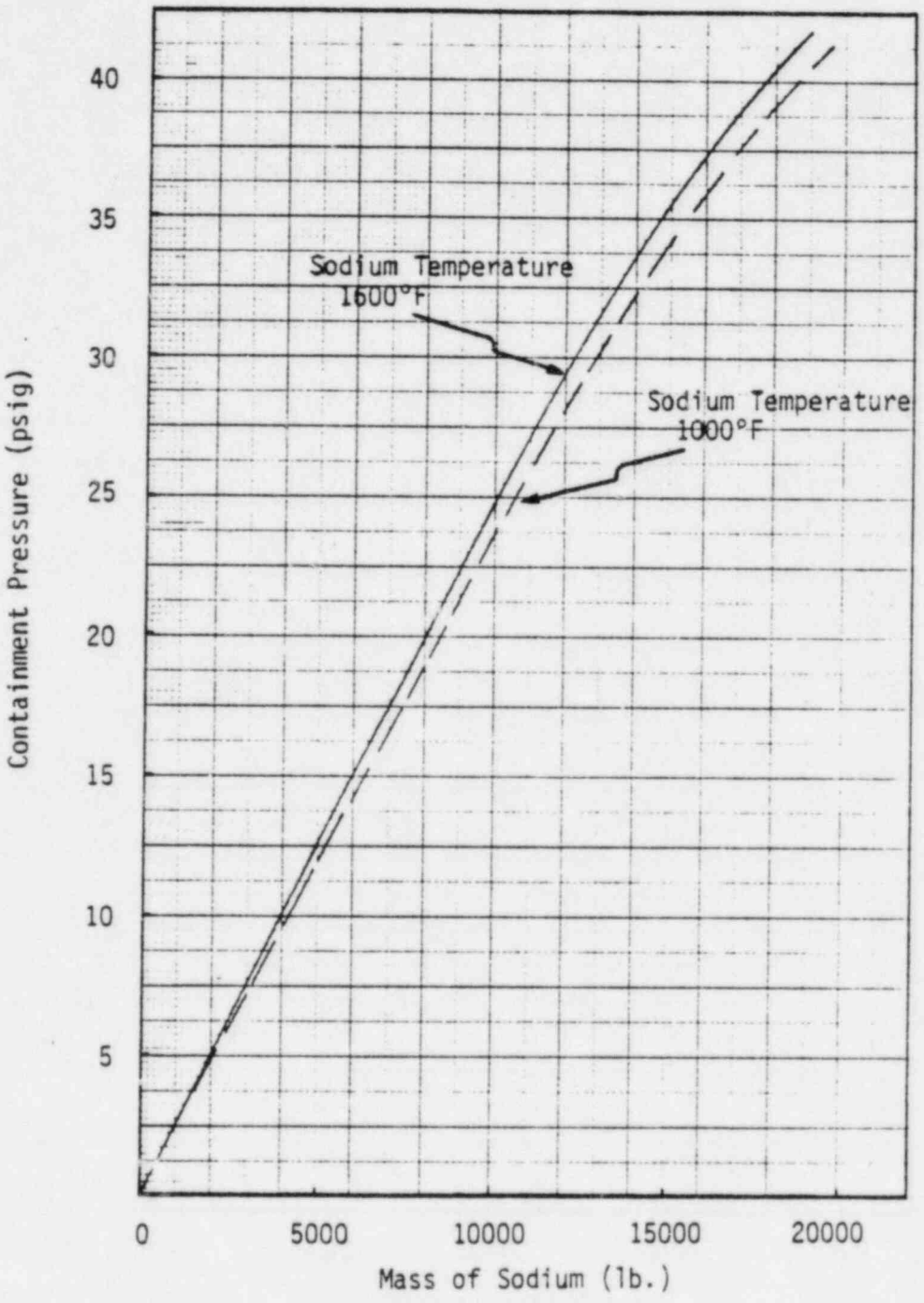

Figure 1: Containment Pressure Resulting from Instantaneous Combustion of Sodium

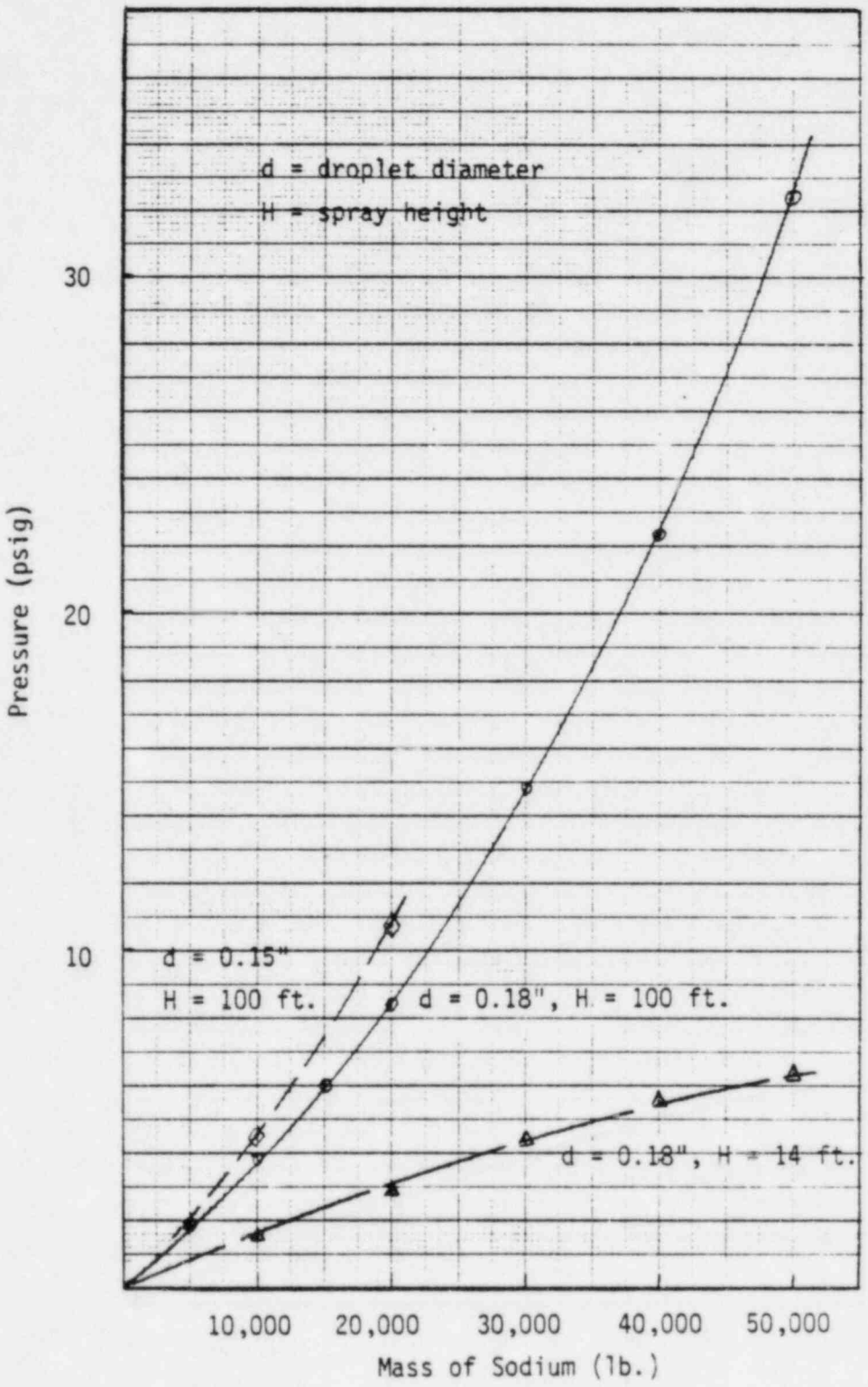

Figure 2: Containment Pressure (from SPRAY analysis)

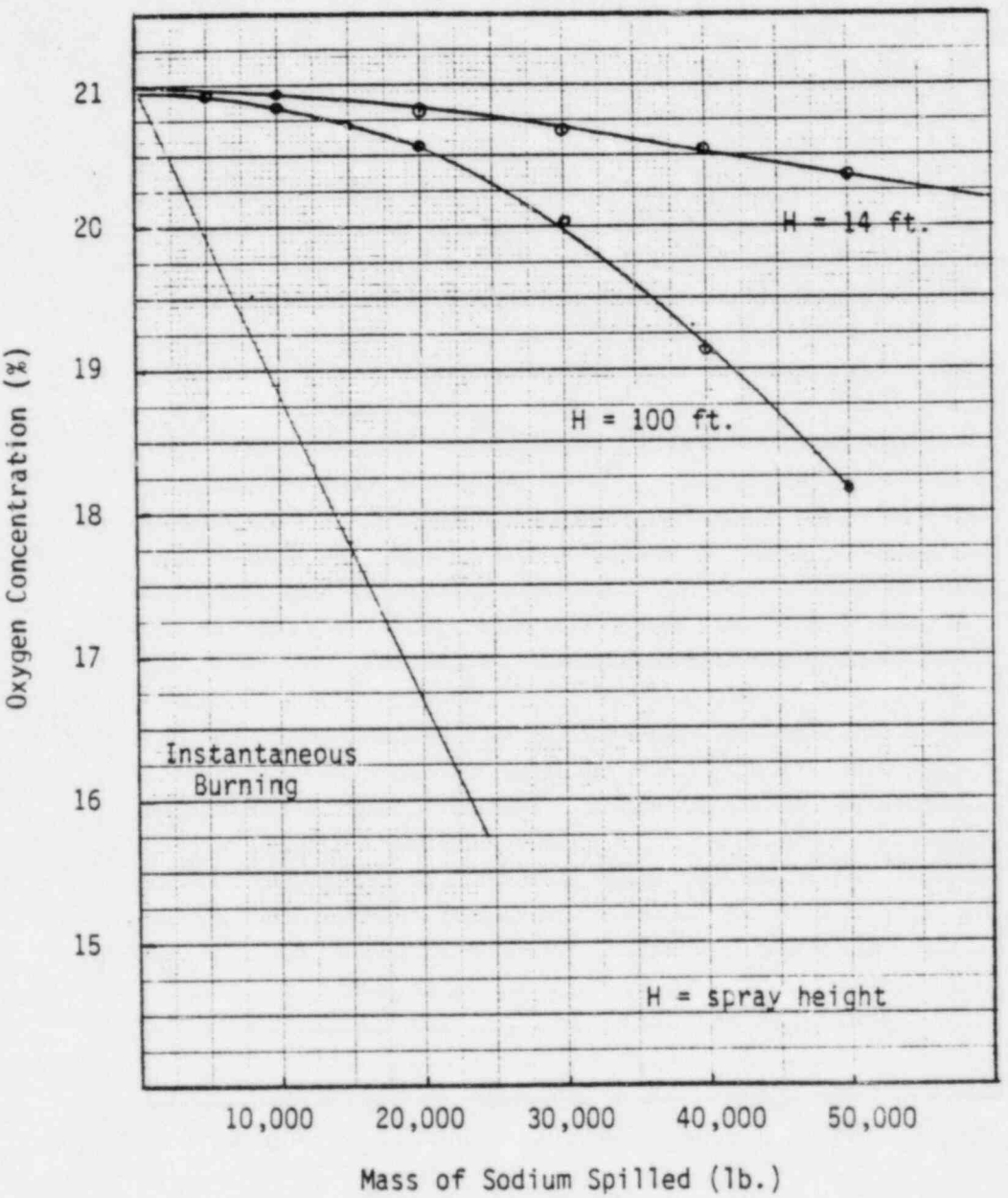

Figure 3: Oxygen Concentration in the RCB

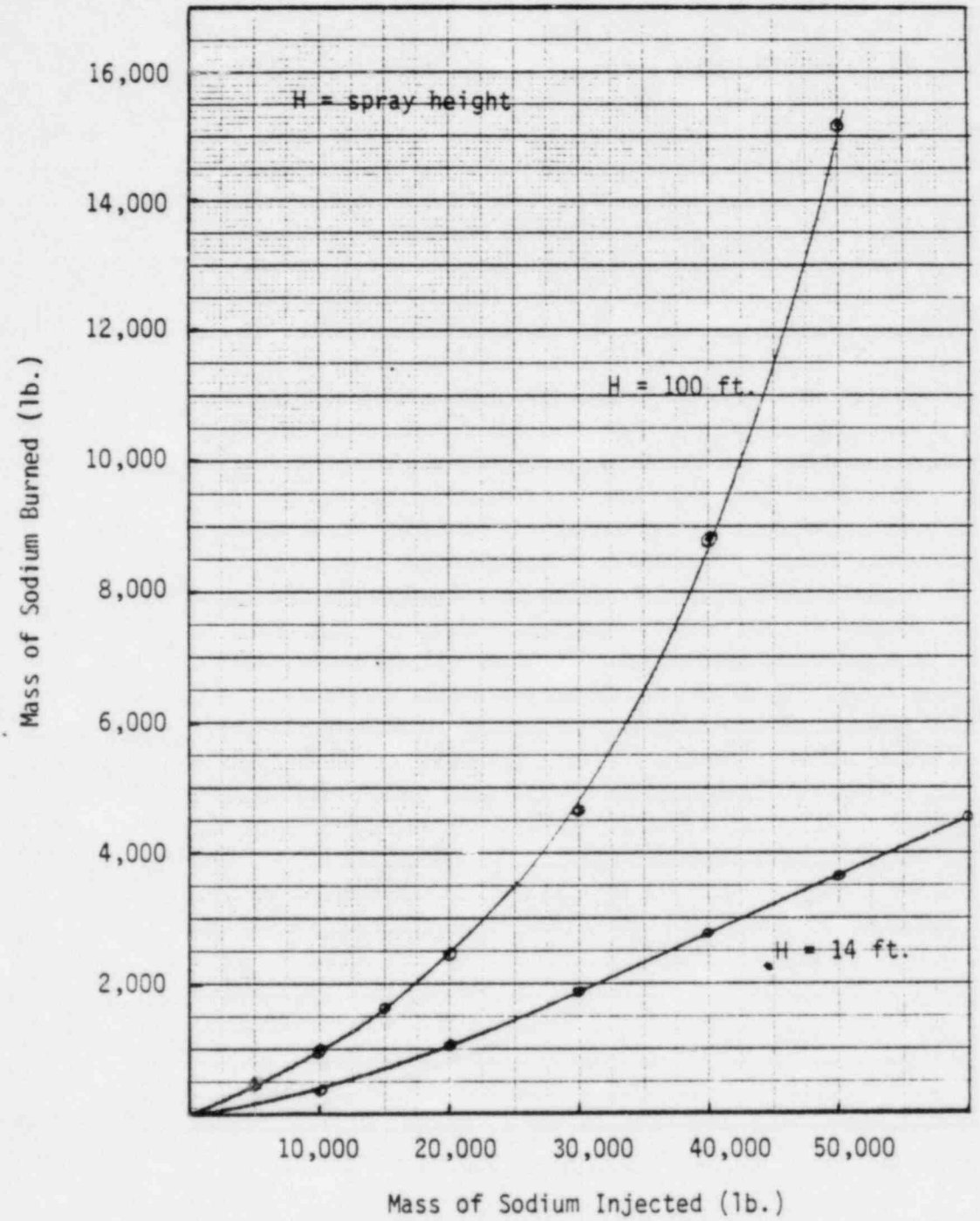

Figure 4: Total Mass of Sodium Burned

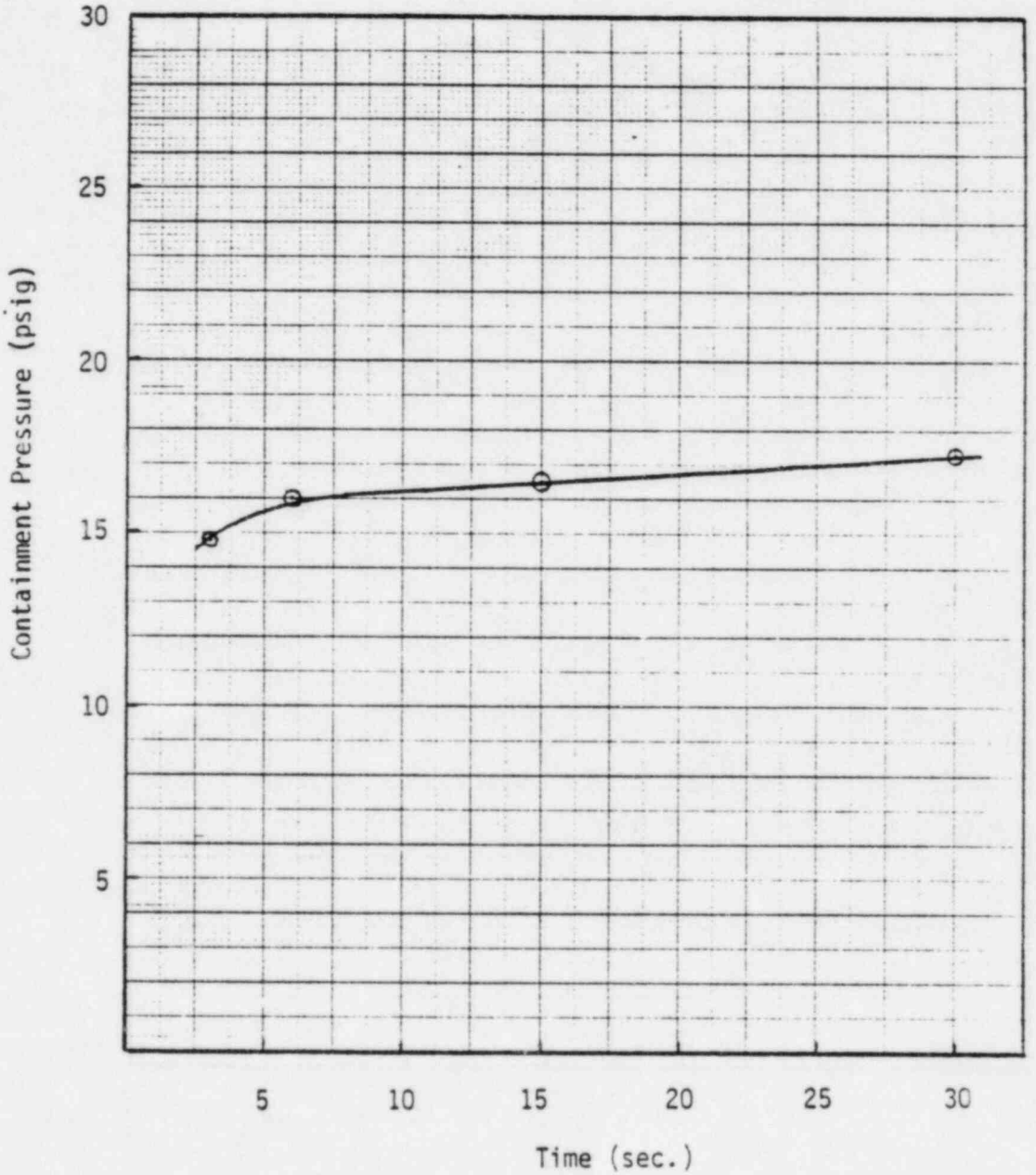

Figure 5: Containment Pressure as a Function of SPRAY Duration (Total mass = 30,000 lbs.)

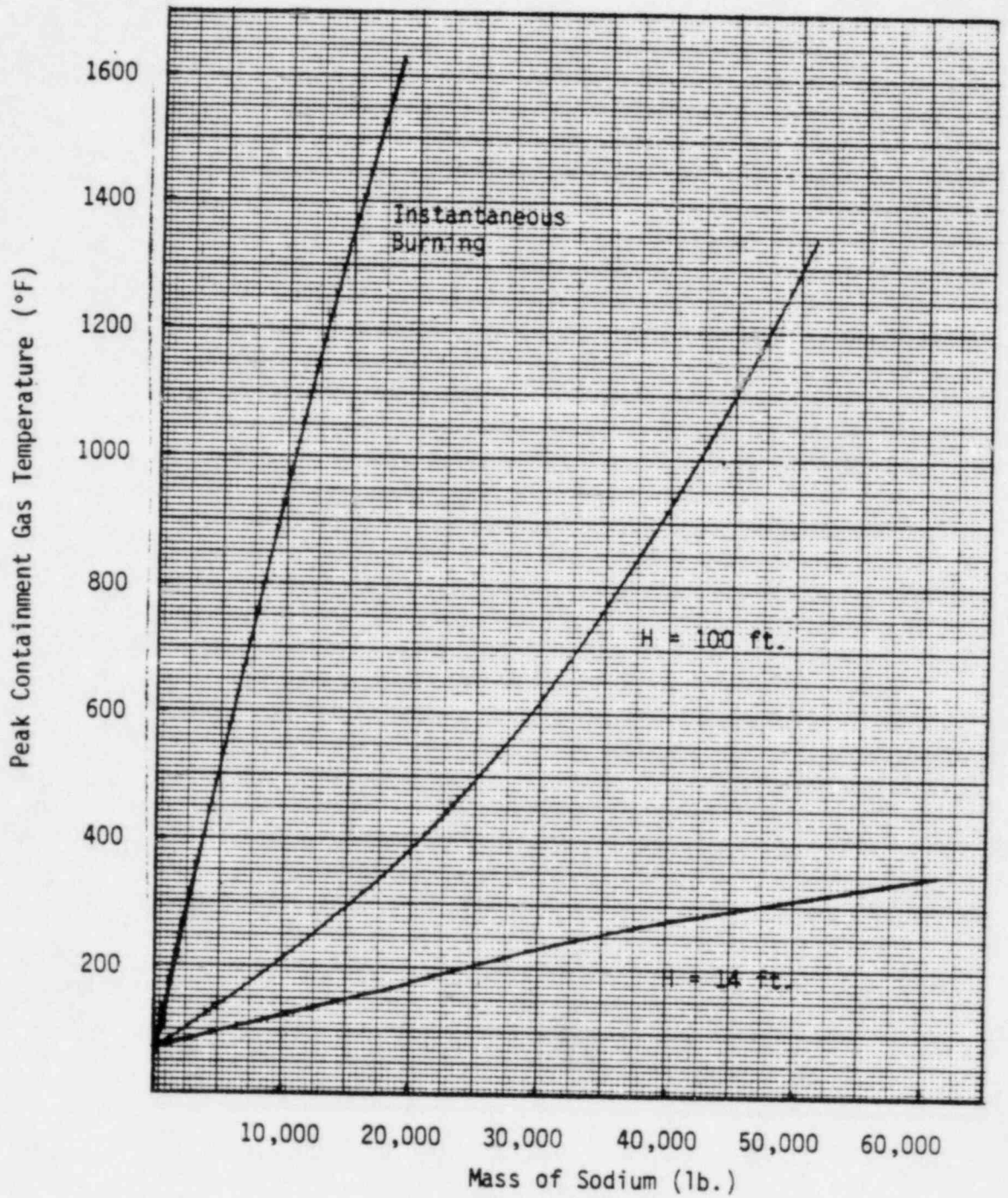

Figure 6: Peak Containment Gas Temperature

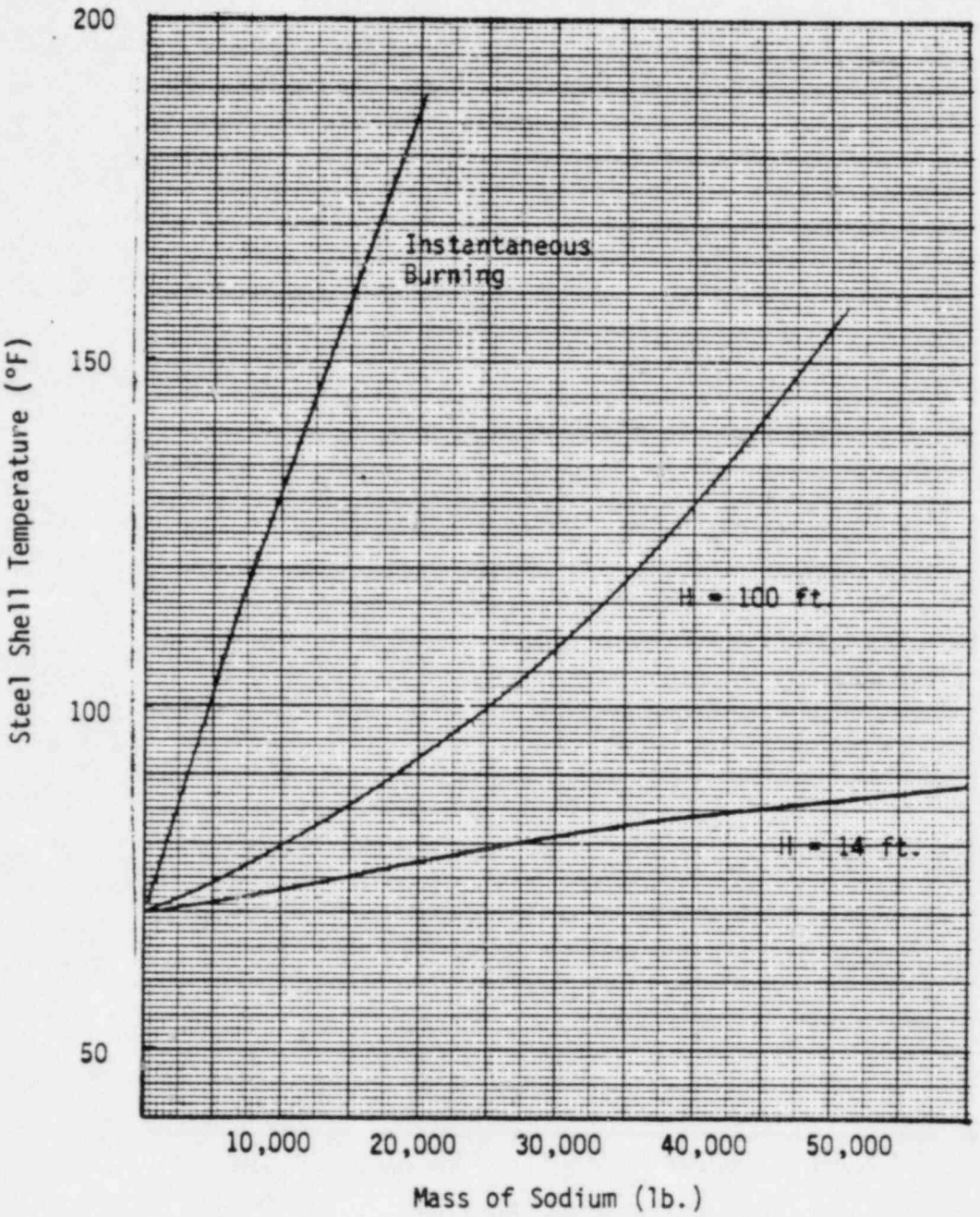

Figure 7: Steel Containment Shell Equilibrium Temperature Resulting from Sprays